

Effect of polyfluorination on ring inversion barriers for cyclooctatetraenes. Transition-metal compounds of unsaturated, polyfluorinated cycloaliphatics. Crystal and molecular structures of [Fe(.eta.-C5R5)(.eta.1-heptafluorocycloocta-1,3,5,7-tetraenyl)(CO)2] (R = H, Me), {[Fe(.eta.-C5H5)(CO)2]2(.mu.2-(1.eta.,5.eta.)-hexafluorocycloocta-1,3,5,7-tetraenediy)}, and [Mn((3.eta.)-heptafluorotricyclo[4.2.0.02,5]octa-3,7-dienyl)(CO)5]

Russell P. Hughes, Richard T. Carl, Stephen J. Doig, Richard C. Hemond, Deborah E. Samkoff, Wayne L. Smith, Leslie C. Stewart, Raymond E. Davis, Katherine D. Holland, and
Organometallics, **1990**, 9 (10), 2732-2745 • DOI: 10.1021/om00160a022 • Publication Date (Web): 01 May 2002

Downloaded from <http://pubs.acs.org> on March 8, 2009

More About This Article

The permalink <http://dx.doi.org/10.1021/om00160a022> provides access to:

- Links to articles and content related to this article
- Copyright permission to reproduce figures and/or text from this article



**Effect of Polyfluorination on Ring Inversion Barriers for
Cyclooctatetraenes. Synthesis of
Heptafluorocycloocta-1,3,5,7-tetraenyl,
Hexafluorocycloocta-1,3,5,7-tetraenediyl,
Heptafluorotricyclo[4.2.0.0^{2,5}]octa-3,7-dienyl, and
Hexafluorotricyclo[4.2.0.0^{2,5}]octa-3,7-dienediyl Transition-Metal
Compounds. Crystal and Molecular Structures of
[Fe(η -C₅R₅)(η ¹-heptafluorocycloocta-1,3,5,7-tetraenyl)(CO)₂]
(R = H, Me), [[Fe(η -C₅H₅)(CO)₂]₂(μ ₂-
(1 η ,5 η)-hexafluorocycloocta-1,3,5,7-tetraenediyl)], and
[Mn((3 η)-heptafluorotricyclo[4.2.0.0^{2,5}]octa-3,7-dienyl)(CO)₅]**

Russell P. Hughes,^{*,1a} Richard T. Carl,^{1a} Stephen J. Doig,^{1a} Richard C. Hemond,^{1a}
Deborah E. Samkoff,^{1a} Wayne L. Smith,^{1a,2} Leslie C. Stewart,^{1a} Raymond E. Davis,^{*,1b}
Katherine D. Holland,^{1b} Pamela Dickens,^{1b} and Ram P. Kashyap^{1b}

*Chemistry Departments, Dartmouth College, Hanover, New Hampshire 03755,
and University of Texas at Austin, Austin, Texas 78712*

Received March 8, 1990

Octafluorocyclooctatetraene (OFCOT; 1) reacts with various transition-metal carbonyl anions to yield the η^1 -heptafluorocyclooctatetraenyl complexes [M(η^1 -C₈F₇)] (M = Mn(CO)₅ (7), Re(CO)₅ (16), Fe(C₅H₅)(CO)₂ (17), Fe(C₅Me₅)(CO)₂ (24), Ru(C₅H₅)(CO)₂ (27)), which in most cases are in dynamic equilibrium with small amounts of their heptafluorobicyclo[4.2.0]octatrienyl valence isomers 12, 18, 25, and 28, respectively. The formation of the bicyclic complex 18 has been shown to occur via initial formation of 17 and subsequent isomerization. The conformational dynamics of the fluorinated rings in these complexes have been examined. In all cases ring inversion with concomitant bond shift isomerization is slow on the NMR time scale. In complex 17 ring inversion has been shown to be slow on the NMR time scale. Complex 17 reacts with EPh₃ (E = P, As) to yield the complexes [Fe(C₅H₅)(η^1 -C₈F₇)(CO)(EPh₃)] (E = P (29), As (30)) as diastereoisomeric pairs that can be separated and that do not interconvert at room temperature. Kinetic investigations of the conversion of one diastereomer of 30 into the other have yielded the activation parameters $E_a = 23.0(\pm 0.9)$ kcal mol⁻¹, $\ln A = 26.1(\pm 1.4)$, $\Delta G^\ddagger = 24.4(\pm 0.3)$ kcal mol⁻¹, $\Delta H^\ddagger = 22.4(\pm 0.9)$ kcal mol⁻¹, and $\Delta S^\ddagger = -6.6(\pm 1.8)$ eu; these have been shown to represent minimum values for the inversion of the fluorinated ring. Comparison of the ΔG^\ddagger value for 30 with that for ring inversion of a hydrocarbon analogue indicates that fluorination of the ring increases ΔG^\ddagger for this process by ≥ 7.1 kcal mol⁻¹. The fluorinated ring in the monosubstituted complex 17 reacts with a further 1 equiv of [Fe(C₅H₅)(CO)₂]⁻ to yield the disubstituted ring compound 22. The valence isomer of OFCOT *anti*-perfluorotricyclo[4.2.0.0^{2,5}]octa-3,7-diene (9) reacts with metal carbonyl anions to afford the mono- and disubstituted compounds 13, 19, 20, and 21. An unusual transformation of the η^1 -heptafluorocyclooctatetraenyl ligand to the pentafluorobenzocyclobutenone ligand has been shown to occur during chromatography. Single-crystals X-ray diffraction studies of complexes 17, 24, 22, and 13 have been carried out. X-ray data were collected on a Syntex P2₁ autodiffractometer at -110 °C, and structures were refined by the full-matrix least-squares method. For 17, $a = 21.390(5)$ Å, $b = 7.507(1)$ Å, $c = 18.767(5)$ Å, $\beta = 108.63(2)^\circ$, monoclinic, $C2/c$, $Z = 8$, $R = 0.053$, and $R_w = 0.050$ for 2660 reflections with $F_o \geq 4\sigma(F_o)$. For 24, $a = 15.307(4)$ Å, $b = 13.952(3)$ Å, $c = 9.058(2)$ Å, $\beta = 92.01(2)^\circ$, monoclinic, $P2_1/n$, $Z = 4$, $R = 0.036$, and $R_w = 0.034$ for 3612 reflections with $F_o \geq 4\sigma(F_o)$. For 22, $a = 11.317(2)$ Å, $b = 11.458(2)$ Å, $c = 8.006(2)$ Å, $\alpha = 99.13(1)^\circ$, $\beta = 91.04(1)^\circ$, $\gamma = 93.63(1)^\circ$, triclinic, $P\bar{1}$, $Z = 2$, $R = 0.052$, and $R_w = 0.061$ for 4495 reflections with $F_o \geq 4\sigma(F_o)$. For 13, $a = 12.131(2)$ Å, $b = 8.491(1)$ Å, $c = 14.892(2)$ Å, $\beta = 112.05(2)^\circ$, monoclinic, $P2_1/c$, and $Z = 4$; a disordered model in which the bicyclic fluorocarbon ring appears in two orientations has been refined to $R = 0.046$ and $R_w = 0.043$ for 3422 reflections with $F_o \geq 4\sigma(F_o)$.

Introduction

Cyclooctatetraene (COT) is the smallest nonplanar 4n annulene and has been a historically important ligand in the development of the organometallic chemistry of the

d-block and f-block elements.³ Our studies of the transition-metal chemistry of its perfluorinated analogue octafluorocyclooctatetraene (OFCOT; 1)^{4,5} have revealed

(1) (a) Dartmouth College. (b) University of Texas at Austin.
(2) ACS-PRF Summer Faculty Fellow on sabbatical leave from the Chemistry Department, Colby College, Waterville, ME 04901.

(3) For reviews of the organic and organometallic chemistry of cyclooctatetraene see: (a) Fray, G. I.; Saxton, R. G. *The Chemistry of Cyclooctatetraene and Its Derivatives*; Cambridge University Press: Cambridge, England, 1978. (b) Deganello, G. *Transition Metal Complexes of Cyclic Polyolefins*; Academic Press: New York, 1979.

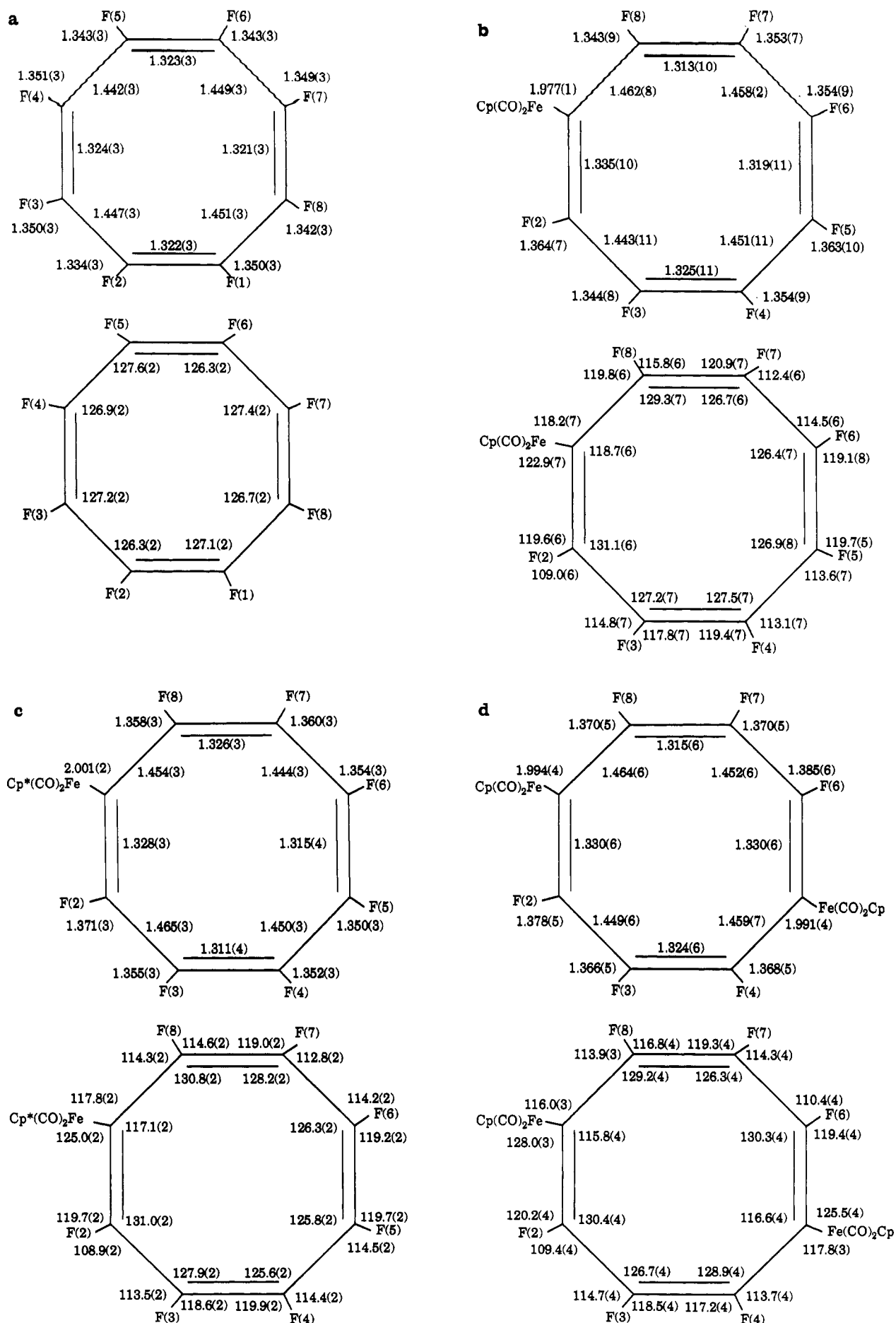
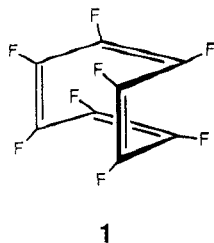
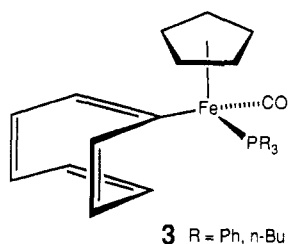


Figure 1. Bond lengths (Å) and angles (deg) for the fluorinated rings in (a) OFCOT, (b) complex 17, (c) complex 24, and (d) complex 22. Values for C-C lengths and C-C-C angles appear inside the ring. Values for C-F lengths and C-C-F angles appear outside the ring.



coordination chemistry significantly different from that of COT, and we have characterized examples of 1,2- η ,^{6,7} 1,4- η ,⁸ 1,2,5,6- η ,⁸⁻¹¹ 1,2,3,6- η ,^{6,8,9} and 1-6 η complexes,¹² as well as valence isomeric η^4 -bicyclo[4.2.0]octa-2,4,7-triene¹⁰ and η^2 -bicyclo[3.3.0]octadienediy^{18,9,13} compounds derived from this perfluorinated ligand.

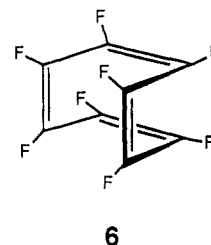
Very few cyclooctatetraenyl complexes are known in which the metal is attached to the organic ring framework via a σ bond to carbon. The racemic iron compound **2** has been prepared either by reaction of cyclooctatetraenyl-lithium with $\text{FpI}^{14,15}$ or of bromocyclooctatetraene with the Fp^- anion¹⁵ ($\text{Fp} = \text{Fe}(\eta\text{-C}_8\text{H}_5)(\text{CO})_2$), and its diastereoisomeric phosphine derivative **3** (only one diastereoisomer is



shown) have been synthesized by photochemical replacement of a CO ligand in **2** by PR_3 .¹⁵ Compound **2** exists as two enantiomers by virtue of the conformational asymmetry of the monosubstituted cyclooctatetraene ring, and **3** exists as a diastereoisomeric mixture due to the additional asymmetric center at iron. In such monosubstituted systems two important isodynamic phenomena are possible due to the nonplanarity of the ring and the alternating single and double bonds (see Scheme I).¹⁶ Provided that

these processes occur at suitable rates, they can be monitored by NMR spectroscopic techniques. The first process, ring inversion (RI), interconverts enantiomers such as **2a** and **2b** through the presumably planar intermediate **4**. This process does not give rise to intramolecular site exchange of ring carbon atoms (or their substituents), but its operation is manifested in the ¹³C NMR spectrum by site exchange of diastereotopic carbonyl sites (CO_A and CO_B) on the metal atom. Second, during the lifetime of **4** a bond shift isomerization (BS) process may also occur, via the transition state **5**. This does give rise to site exchange within the cyclooctatetraene ring, interconverting positions 2 with 8, 3 with 7, and 4 with 6, and can be monitored by observing the coalescence of the appropriate NMR resonances. For compounds such as **2**, RI with or without BS interconverts enantiomers **2a** and **2b**: for diastereoisomeric pairs such as **3**, RI epimerizes only one chiral center and would interconvert, for example, the RS and RR diastereoisomers, which have different NMR resonances.

For both **2** and **3** values of $\Delta G^\ddagger(\text{RI}) \approx 17$ kcal mol⁻¹ and $\Delta G^\ddagger(\text{BS}) \approx 18$ kcal mol⁻¹ have been determined from NMR measurements.¹⁵ Analogous processes have been studied extensively in cyclooctatetraenes bearing other substituents.¹⁶ By way of comparison, ethoxycyclooctatetraene^{3a,17} has $\Delta G^\ddagger(\text{RI}) = 12.5$ kcal mol⁻¹ and $\Delta G^\ddagger(\text{BS}) = 16.0$ kcal mol⁻¹. Values for other monosubstituted derivatives^{3a} differ by ca. ± 2 kcal mol⁻¹, and more heavily substituted compounds have substantially higher barriers for both processes, due to steric buttressing effects in the planar intermediate.¹⁶ Thus, while the transition-metal substituent in **2** or **3** does increase the barriers for RI and BS relative to those for smaller substituents, this effect is not large enough to prevent observation of both these processes on the NMR time scale.¹⁵ At the outset of this work the effect of polyfluorination on the energetics of these isodynamic processes had not been evaluated. Recently the kinetic parameters of the isodynamic bond shift process in 1,2,3,4,5,6,7-heptafluorocycloocta-1,3,5,7-tetraene (**6**)



were determined with use of a ¹⁹F NMR spin saturation transfer experiment. The saturation transfer experiment was performed at four different temperatures and afforded $E_{a,\text{BS}} = 20 (\pm 0.9)$ kcal mol⁻¹ and $\Delta H^\ddagger_{\text{BS}} = 21.1 (\pm 0.9)$ kcal mol⁻¹. The difference in BS activation energy for heptafluorocyclooctatetraene relative to that for the parent molecule cyclooctatetraene ($\Delta E_a = 10.6$ kcal mol⁻¹) was ascribed to steric effects due to buttressing of the slightly larger fluorine atoms on going from the tub form to the planar delocalized intermediate.¹⁸

The known reactions of fluorinated olefins, arenes, and heterocycles with metal carbonyl anions, to afford fluoro-vinyl or fluoroaryl complexes resulting from net displacement of fluoride ion,¹⁹ prompted us to attempt such

(4) Lemal, D. M.; Buzby, J. M.; Barefoot, A. C., III; Grayston, M. W.; Laganis, E. D. *J. Org. Chem.* **1980**, *45*, 3118-3120.

(5) Laird, B. B.; Davis, R. E. *Acta Crystallogr. Sect. B* **1982**, *B38*, 678-680.

(6) Barefoot, A. C., III; Corcoran, E. W., Jr.; Hughes, R. P.; Lemal, D. M.; Saunders, W. D.; Laird, B. B.; Davis, R. E. *J. Am. Chem. Soc.* **1981**, *103*, 970.

(7) The structure of $[\text{Fe}(\eta^2\text{-C}_8\text{F}_7)(\text{CO})_4]$ has now been verified crystallographically: Davis, R. E. Unpublished results.

(8) Hughes, R. P.; Carl, R. T.; Hemond, R. C.; Samkoff, D. E.; Rheingold, A. L. *J. Chem. Soc., Chem. Commun.* **1986**, 306-308.

(9) Hughes, R. P.; Samkoff, D. E.; Davis, R. E.; Laird, B. B. *Organometallics* **1983**, *2*, 195-197.

(10) Doherty, N. M.; Ewels, B. E.; Hughes, R. P.; Samkoff, D. E.; Saunders, W. D.; Davis, R. E.; Laird, B. B. *Organometallics* **1985**, *4*, 1606-1611.

(11) Carl, R. T.; Doig, S. J.; Geiger, W. E.; Hemond, R. C.; Hughes, R. P.; Kelly, R. S.; Samkoff, D. E. *Organometallics* **1987**, *6*, 611.

(12) Examples of 1-6 η complexes include $[\text{Mn}(\text{C}_8\text{R}_8)(\eta^1\text{-C}_8\text{F}_8)]$ (R = H, Me), both of which have been crystallographically characterized: Hemond, R. C.; Hughes, R. P.; Rheingold, A. L. *Organometallics* **1989**, *8*, 1261-1269.

(13) Hughes, R. P.; Carl, R. T.; Samkoff, D. E.; Davis, R. E.; Holland, K. D. *Organometallics* **1986**, *5*, 1053-1055.

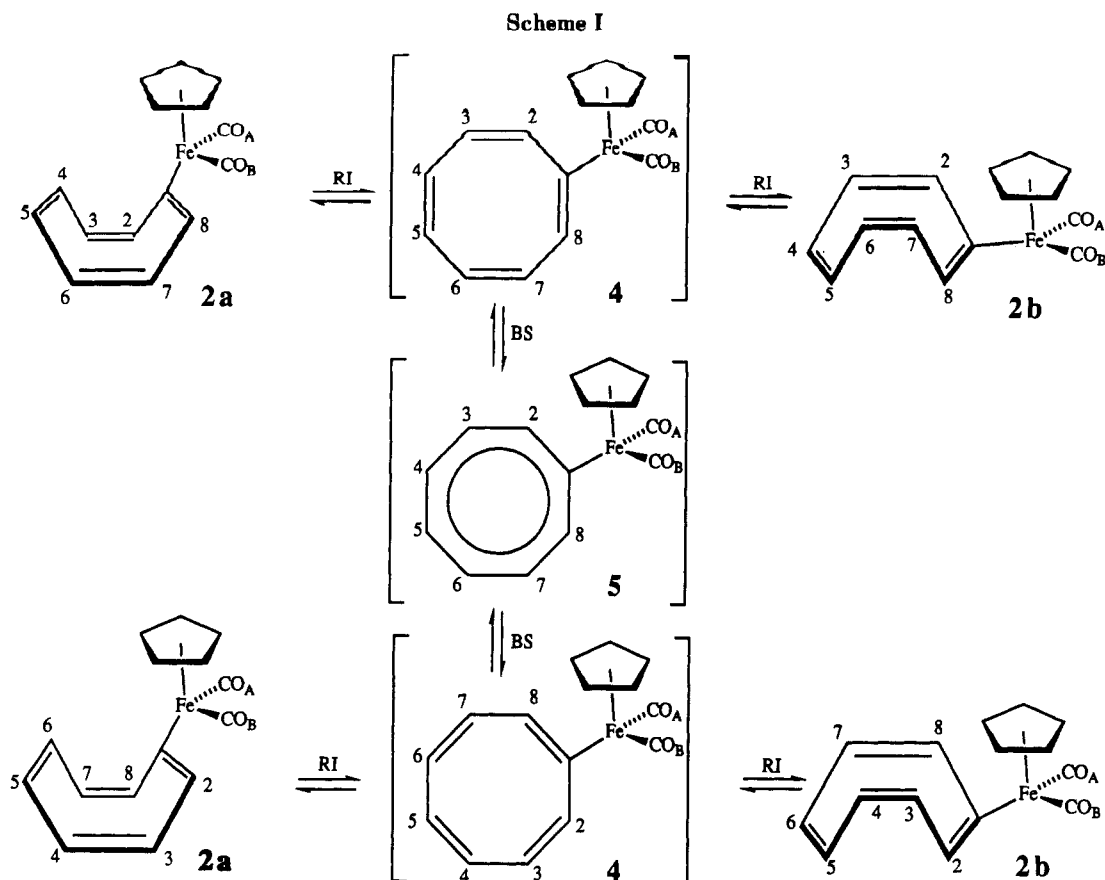
(14) Cooke, M.; Russ, C. R.; Stone, F. G. A. *J. Chem. Soc., Dalton Trans.* **1975**, 256.

(15) Radcliffe, M. D.; Jones, W. M. *Organometallics* **1983**, *2*, 1053-1055.

(16) For a recent review of these phenomena, see: Paquette, L. A. *Pure Appl. Chem.* **1982**, *54*, 987-1004 and references cited therein.

(17) Oth, J. F. M. *Pure Appl. Chem.* **1971**, *25*, 573.

(18) Lemal, D. M.; Spector, T. Private Communication to R. P. Hughes.

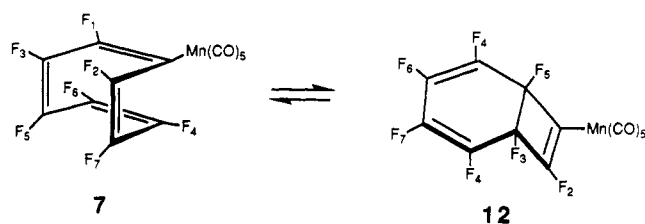


substitution reactions with OFCOT, in the hope of generating metal-substituted heptafluorocyclooctatetraenes. This paper describes in full our synthetic, dynamic, and X-ray structural studies on the products of these and related reactions. Parts of this work have been subject of preliminary communications.^{20,21}

Results and Discussion

Reactions of $\text{Na}^+[\text{M}(\text{CO})_5]^-$ ($\text{M} = \text{Mn, Re}$) with OFCOT and *anti*-Octafluorotricyclo[4.2.0.0^{2,5}]octa-3,7-diene. The room-temperature reaction of $\text{Na}^+[\text{Mn}(\text{CO})_5]^-$ with a slight excess of OFCOT afforded a yellow solution whose ^{19}F NMR spectrum exhibited seven major resonances as well as seven minor signals (ca. 10% of the intensity of the major peaks). Column chromatography on Florisil, followed by low-temperature crystallization, afforded a white, air-stable solid. The solution infrared

spectrum of this material exhibited five bands in the metal carbonyl region, characteristic of an $\text{Mn}(\text{CO})_5$ group σ -bonded to a fluorocarbon ligand.^{19b} Its ^{19}F NMR spectrum displayed the same two sets of seven resonances in a ratio identical with that observed in the crude reaction mixture. As shown in Table I, the seven major resonances were attributed to the heptafluorocyclooctatetraenyl complex 7, on the basis of a comparison of its ^{19}F NMR chemical shift and coupling constant data with those of 1,2,3,4,5,6,7-heptafluorocycloocta-1,3,5,7-tetraene (6), which has been characterized by $^{19}\text{F}\{^{19}\text{F}\}$ NMR and magnetization transfer experiments.¹⁸



The experimental observation that the ratio of 7 to the minor product was unaffected by recrystallization, followed by dissolution at room temperature, suggested the presence of an equilibrium in solution between the η^1 -heptafluorocyclooctatetraenyl ligand and a valence isomer. Two known valence isomers of OFCOT are perfluorobicyclo[4.2.0]octa-2,4,7-triene (8)²² and perfluorotricyclo[4.2.0.0^{2,5}]octa-3,7-diene (9).²³ The tricyclic isomer 9 is not in thermal equilibrium with OFCOT,²³ while the amount of 8 in equilibrium with OFCOT is extremely small ($K_{\text{eq}} = [8]/[1] = 0.003$ (20 °C, acetone- d_6)).²² However,

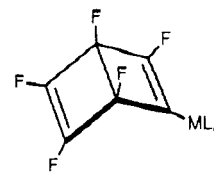
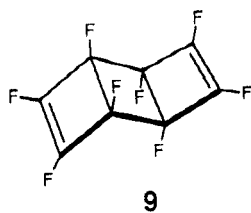
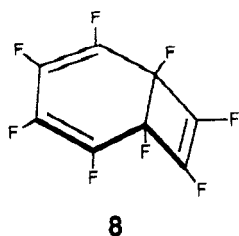
(19) (a) Jolly, P. W.; Bruce, M. I.; Stone, F. G. A. *J. Chem. Soc.* 1965, 5830. (b) Bruce, M. I.; Jolly, P. W.; Stone, F. G. A. *J. Chem. Soc. A* 1966, 1602. (c) Bruce, M. I.; Stone, F. G. A. *Angew. Chem., Int. Ed. Engl.* 1968, 7, 747. (d) Cooke, D. J.; Green, M.; Mayne, N.; Stone, F. G. A. *J. Chem. Soc. A* 1968, 1771. (e) Booth, B. L.; Haszeldine, R. N.; Tucker, N. I. *J. Organomet. Chem.* 1968, 11, 5. (f) Cullen, W. R. *Fluorine Chem. Rev.* 1969, 3, 73. (g) Booth, B. L.; Haszeldine, R. N.; Perkins, I. *J. Chem. Soc. A* 1971, 937. (h) Bruce, M. I.; Goodall, B. L.; Sharrocks, D. N.; Stone, F. G. A. *J. Organomet. Chem.* 1972, 49, 139. (i) Bennett, R. L.; Bruce, M. I.; Gardner, R. C. F. *J. Chem. Soc., Dalton Trans.* 1973, 2653. (j) Booth, B. L.; Haszeldine, R. N.; Taylor, M. B. *J. Chem. Soc. A* 1970, 1974. (k) Booth, B. L.; Haszeldine, R. N.; Perkins, I. *J. Chem. Soc., Dalton Trans.* 1975, 1843. (l) Booth, B. L.; Haszeldine, R. N.; Perkins, I. *J. Chem. Soc., Dalton Trans.* 1975, 1847. (m) Booth, B. L.; Casey, S.; Haszeldine, R. N. *J. Organomet. Chem.* 1982, 226, 289. (n) Booth, B. L.; Casey, S.; Critchley, R. P.; Haszeldine, R. N. *J. Organomet. Chem.* 1982, 226, 301. (o) Artamkina, G. A.; Mil'chenko, A. Yu.; Beletskaya, I. P.; Reutov, O. A. *J. Organomet. Chem.* 1986, 311, 199. (p) Bruce, M. I.; Liddell, M. J.; Snow, M. R.; Tiekink, E. R. T. *J. Organomet. Chem.* 1988, 354, 103-115.

(20) Doig, S. J.; Hughes, R. P.; Patt, S. L.; Samkoff, D. E.; Smith, W. L. *J. Organomet. Chem.* 1983, 250, C1-C4.

(21) Doig, S. J.; Hughes, R. P.; Davis, R. E.; Gadol, S. M.; Holland, K. D. *Organometallics* 1984, 3, 1921-1922.

(22) Waldron, R. F.; Barefoot, A. C., III; Lemal, D. M. *J. Am. Chem. Soc.* 1984, 106, 8301-8302.

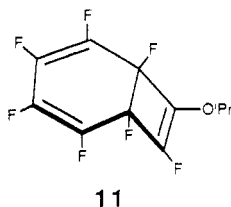
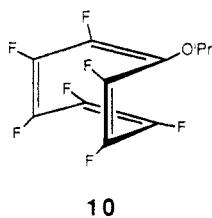
(23) Barefoot, A. C., III; Saunders, W. D.; Buzby, J. M.; Grayston, M. W.; Lemal, D. M. *J. Org. Chem.* 1980, 45, 4292-4295.



14 $ML_n = \text{Re}(\text{CO})_5$

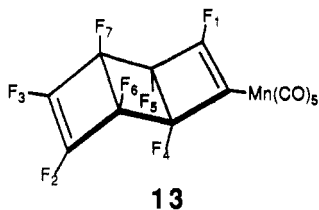
15 $ML_n = \text{Fe}(\text{C}_5\text{H}_5)(\text{CO})_2$

a recent investigation of the solution dynamics of 1,2,3,4,5,6,7-heptafluoro-8-isopropoxycycloocta-1,3,5,7-tetraene (10) has shown that the presence of a σ -bonded isopropoxy group can have a dramatic effect on K_{eq} . The corresponding equilibrium constant ($K_{\text{eq}} = [10]/[11] = 1.09$ (20 °C)) is 360 times greater than that between OFCOT and 8.²⁴



Accordingly the minor product of the reaction of OFCOT with $[\text{Mn}(\text{CO})_5]^-$ was assigned the bicyclic structure 12; thus, at 20 °C, $K_{\text{eq}} = [12]/[7] \approx 0.1$. The assignment of the signals in the ^{19}F NMR spectrum of 12 (Table II) was accomplished by a comparison of the fluorine-fluorine coupling constants and chemical shifts with those of 8²² and 11.²⁴ The dynamic nature of this equilibrium has been confirmed for an analogous system discussed below.

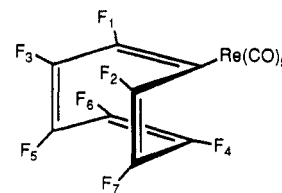
Further indirect confirmation of the structure of 12 was made by the unambiguous synthesis and characterization of the monosubstituted tricyclic complex 13, by the room-temperature reaction of $\text{Na}^+[\text{Mn}(\text{CO})_5]^-$ with 9 in THF. The solid-state structure of 13 was also confirmed



by a single-crystal X-ray diffraction study (see below). The solution structure of 13 was determined by infrared and ^{19}F NMR spectroscopy to be identical with that observed in the solid state, with the perfluorinated ligand in the anti configuration and the metal center σ -bound to one olefinic carbon. The ^{19}F NMR spectrum of 13 (Table III) exhibited seven signals of equal intensity that were clearly not those observed for 12 (Table II). As observed for 7, the IR spectrum of 13 displayed five M-CO bands characteristic of an $\text{Mn}(\text{CO})_5$ group σ -bonded to an asymmetric fluoro-carbon ligand.^{19b} IR bands were also observed at 1755 and 1609 cm^{-1} , which were assigned to the $\text{FC}=\text{CF}$ and $\text{Mn}-\text{C}=\text{CF}$ groups on the basis of a comparison with similar complexes; e.g. in 14, the corresponding bands are observed at 1735 cm^{-1} ($\nu_{\text{FC}=\text{CF}}$) and 1605 cm^{-1} ($\nu_{\text{Re}-\text{C}=\text{CF}}$), while in 15 they appear at 1740 cm^{-1} ($\nu_{\text{FC}=\text{CF}}$) and 1603 cm^{-1} ($\nu_{\text{Fe}-\text{C}=\text{CF}}$).^{19c}

Curiously, the room-temperature reaction of $\text{Na}^+[\text{Re}(\text{CO})_5]^-$ with OFCOT afforded only the monocyclic complex

16. No evidence for the formation of a bicyclic valence



16

isomer was observed in the ^{19}F NMR spectrum (Table I) of either the crude reaction residue or the recrystallized sample. As observed for 7 and 13, the infrared spectrum of 16 exhibited five bands in the metal carbonyl region characteristic of an $\text{Re}(\text{CO})_5$ group σ -bonded to a fluoro-carbon ligand.^{19b}

Observation of an apparent equilibrium between the bicyclic isomer 12 and the monocyclic isomer 7 raised the question of whether 12 was formed by a kinetically faster attack of the nucleophilic metal anion on the small amount of bicyclic isomer 8 known to be in equilibrium with OFCOT at room temperature (see above) or whether nucleophilic attack on the OFCOT ring occurred initially to form 7, which then underwent valence isomerization to afford 12. A low-temperature synthesis might distinguish between these two routes for formation of 12. Unfortunately, the nucleophilicity of $[\text{Mn}(\text{CO})_5]^-$ is insufficient to displace fluoride from OFCOT at -78 °C, precluding such a study. However, as discussed below, the low-temperature reaction of the more nucleophilic anion $[\text{Fe}(\eta^5-\text{C}_5\text{H}_5)(\text{CO})_2]^-$ ²⁵ with OFCOT afforded an insight into the formation of these bicyclic isomers.

Since the room temperature ^{19}F NMR spectra of 7 and 16 both display seven resonances, a rapid BS process for these complexes on the NMR time scale is clearly ruled out. Furthermore, no line broadening or magnetization transfer was observed at 80 °C. Also consistent with these results is the observation of eight resonances for the cyclooctatetraene ring carbon atoms in the $^{13}\text{C}\{^{19}\text{F}\}$ NMR spectrum of 16. Two metal carbonyl signals at δ 179.37 (CO_{trans}) and δ 179.68 (CO_{cis}) were also observed in the $^{13}\text{C}\{^{19}\text{F}\}$ NMR spectrum of 16, indicating stereochemical rigidity at the metal center on the NMR time scale. The carbonyl signals could not be observed clearly in the $^{13}\text{C}\{^1\text{H}\}$ NMR spectrum due to coupling to fluorines. However, this result does not provide any information about the isodynamic RI process, due to the absence of diastereotopic groups on the metal. Consequently, the corresponding reactions of OFCOT with the $[\text{M}(\eta^5-\text{C}_5\text{R}_5)(\text{CO})_2]^-$ anions were examined.

Reactions of $[\text{M}(\eta^5-\text{C}_5\text{R}_5)(\text{CO})_2]^-$ ($\text{M} = \text{Fe}, \text{R} = \text{H}, \text{Me}; \text{M} = \text{Ru}, \text{R} = \text{H}$) with OFCOT and anti-Octafluorotricyclo[4.2.0.0^{2,5}]octa-3,7-diene. The reaction of $\text{K}^+[\text{Fe}(\eta^5-\text{C}_5\text{H}_5)(\text{CO})_2]^-$ with OFCOT was carried out in an NMR tube at -78 °C, at which temperature the ^{19}F NMR

(24) Lemal, D. M.; Spector, T. I.; Jensen, B. Unpublished observations communicated to R. P. Hughes.

(25) Dessy, R. D.; Pohl, R. L.; King, R. B. *J. Am. Chem. Soc.* 1966, 88, 5121-5124.

Table I. Comparison of the ^{19}F NMR Chemical Shift Data for (Heptafluorocyclooctatetraenyl)metal Complexes^a ($[[\text{M}](\eta^1\text{-C}_8\text{F}_7)]$)

	[M]	F ₁	F ₂	F ₃	F ₄	F ₅	F ₆	F ₇
6	H	109.2	97.6	132.8	121.9	121.9	126.1	125.2
10	OCH(Me) ₂	124.2	118.8	120.3	125.9	127.0	124.8	127.0
7	Mn(CO) ₅	67.1	93.9	119.9	125.7	127.8	130.1	141.3
16	Re(CO) ₅	65.1	93.6	120.5	125.2	127.8	129.7	142.2
17	FeCp(CO) ₂	74.5	93.8	119.0	124.8	129.0	130.8	140.3
24	FeCp*(CO) ₂ ^d	75.6	93.4	117.9	124.2	129.7	130.8	144.5
27	RuCp(CO) ₂ ^e	72.2	92.7	119.4	125.1	128.8	130.2	143.4
30a	FeCp(AsPh ₃)(CO)	71.9	87.5	117.9	121.5	128.3	130.5	145.8
30b	FeCp(AsPh ₃)(CO)	69.3	90.0	118.2	122.3	130.1	131.7	144.6
	Co(CO) ₃ (PPh ₃) ^e	73.4	94.5	120.2	125.0	128.7	130.9	142.2
	Co(CO) ₃ (P(tol) ₃) ^{b,e}	73.9	94.1	120.2	125.0	129.1	130.1	142.8
	Co(CO) ₃ (PMe ₂ Ph) ^e	73.9	94.5	120.1	125.1	129.1	130.9	142.2
	Co(CO) ₃ (PMe ₃) ^e	72.8	90.0	116.2	122.6	130.4	131.2	147.4
	Co(CO) ₃ (PMePh ₂) ^e	73.8	94.6	120.2	125.2	129.1	131.0	142.5

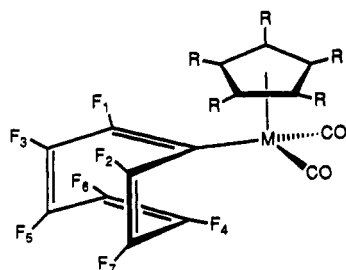
^a Shifts quoted in ppm upfield of CFC1₃. ^b P(tol)₃ = P(*p*-MeC₆H₄)₃. ^c ^{19}F NMR coupling constant data (Hz) for 27: $J_{1,3} = 18$; $J_{3,5} = 25$; $J_{5,6} = 22$; $J_{4,6} = 38$; $J_{4,7} = 23$; $J_{2,7} = 17$; $J_{2,5} = 12$; $J_{3,7} = 11$; $J_{1,4} = 12$; $J_{2,3} = 4$; $J_{5,7} = 3$. All other complexes exhibited very similar coupling constants. ^d Cp* = pentamethylcyclopentadienyl. ^e While the spectra of these cobalt analogues are included here for completeness and convenience, their actual syntheses are described in the following paper in this issue.

Table II. Comparison of the ^{19}F NMR Chemical Shift Data for Bicyclic C₈F₇ Complexes^a ($[[\text{M}](\text{C}_8\text{F}_7)]$)

	[M]	F ₂	F ₃	F ₄	F ₅	F ₆	F ₇
11	OCH(Me) ₂	130.0	153.3	150.0	159.6	157.4	158.7
12	Mn(CO) ₅	93.2	144.3	150.8	155.3	158.7	161.9
18	FeCp(CO) ₂	98.1	144.3	151.0	155.2	159.0	162.8
25	FeCp*(CO) ₂ ^c	98.8	144.5	151.1	155.0	158.6	161.9
28	RuCp(CO) ₂	98.0	145.5	151.6	154.8	158.9	160.9
	Co(CO) ₃ (PPh ₃) ^d	97.4	146.0	151.3	156.2	158.8	160.9
	Co(CO) ₃ (P(tol) ₃) ^{b,d}	98.1	147.1	151.8	155.7	159.3	161.4
	Co(CO) ₃ (PMe ₂ Ph) ^d	97.7	146.5	151.8	156.0	159.0	161.7

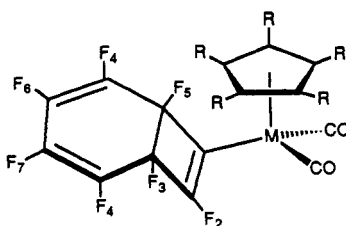
^a Shifts quoted in ppm upfield of internal CFC1₃. ^b P(tol)₃ = P(*p*-MeC₆H₄)₃. ^c Cp* = pentamethylcyclopentadienyl. ^d While the spectra of these cobalt analogues are included here for completeness and convenience, their actual syntheses are described in the following paper in this issue.

spectrum of the crude reaction mixture indicated exclusive formation of the monocyclic complex 17 (see Table I).



17 M = Fe, R = H
24 M = Fe, R = Me
27 M = Ru, R = H

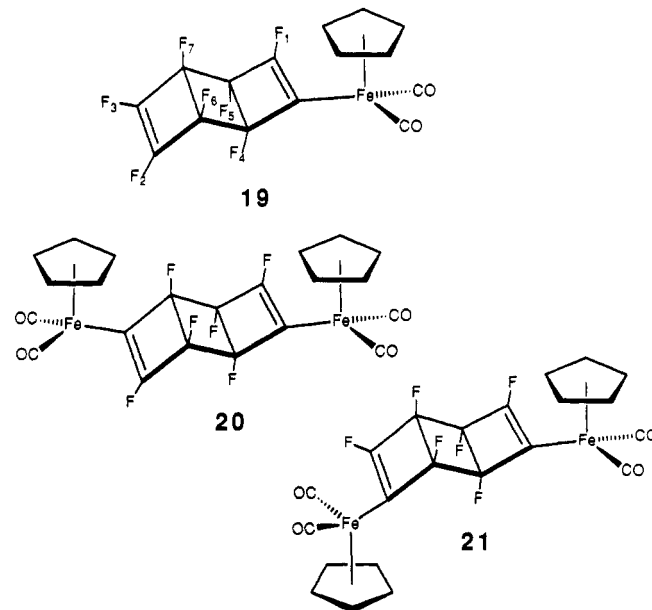
When the solution was warmed to room temperature, seven minor resonances (ca. 10% of the intensity of the major peaks) appeared in addition to those of 17. For reasons discussed above, these resonances were assigned to the bicyclic valence isomer 18 (Table II). Clearly, formation



18 M = Fe, R = H
25 M = Fe, R = Me
28 M = Ru, R = H

of the bicyclic complex occurs solely from valence isomerization of its initially formed monocyclic valence isomer and not from the nucleophilic attack of the transition-metal anion on 8. The equilibrium between 17 and 18 was also shown to be temperature-dependent by allowing solutions to equilibrate over several days at three different temperatures and then recording their ^{19}F NMR spectra. These experiments yielded values of $K_{\text{eq}} = [18]/[17] = 0.13$ (21 °C), 0.15 (1 °C), 0.18 (-55 °C). Recrystallization of these mixtures afforded samples of pure 17, whose solid-state structure was confirmed by a single-crystal X-ray diffraction study (see below).

In contrast to the reaction of $[\text{Mn}(\text{CO})_5]^-$, the reaction of $\text{K}^+[\text{Fe}(\eta^5\text{-C}_5\text{H}_5)(\text{CO})_2]^-$ with the tricyclic fluorocarbon 9 afforded not only the yellow, air-stable, monosubstituted complex 19 but also the disubstituted complexes 20 and 21. The infrared spectrum of 19 displayed two bands in



the metal carbonyl region characteristic of an $\text{M}(\text{CO})_2$ metal center as well as bands at 1757 and 1606 cm^{-1} , which were assigned to the $\text{FC}=\text{CF}$ and $\text{M}-\text{C}=\text{CF}$ groups, respectively. The ^{19}F NMR spectrum of 19 exhibited seven resonances of equal intensity (Table III), which were not isochronous with those observed for 18 (Table II). The unambiguous assignment of the signals in the ^{19}F NMR spectrum of 19 was accomplished through a selective ^{19}F - $\{^{19}\text{F}\}$ decoupling experiment. The solution infrared spec-

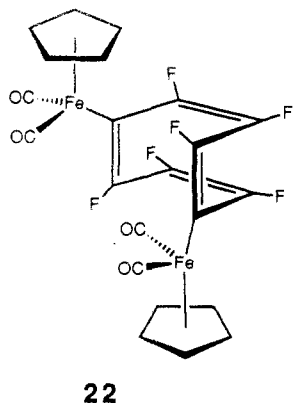
Table III. Comparison of the ^{19}F NMR Chemical Shift Data for 9, 13, 19, 20 and 21^c ($[[\text{M}](\text{C}_5\text{F}_7)]$)

	[M]	F ₁	F ₂	F ₃	F ₄	F ₅	F ₆	F ₇
9	F	125.4	125.4	125.4	181.6	181.6	181.6	181.6
13	Mn(CO) ₅	98.6	120.2	120.4	171.2	180.0	185.9	188.2
19	FeCp(CO) ₂ ^b	103.6	120.5	120.8	168.8	178.6	186.0	188.1
20 ^c	FeCp(CO) ₂	103.0		103.0	170.5	182.1	170.5	182.1
21 ^c	FeCp(CO) ₂	104.7	104.7		172.8	179.7	179.7	172.8

^a Shifts quoted in ppm upfield of internal CFCl_3 . ^b Summary of the ^{19}F NMR coupling constants (Hz) for 19: $J_{1,4} = 7$; $J_{2,3} = 11$; $J_{2,6} = 11$; $J_{2,7} = 4$; $J_{3,5} = 3$; $J_{3,6} = 4$; $J_{3,7} = 15$; $J_{4,5} = 19$; $J_{4,6} = 7$; $J_{5,7} = 4$; $J_{6,7} = 15$. ^c The assignments for these isomers may be reversed.

trum of a mixture of 20 and 21 also displayed two bands in the metal carbonyl region at 2048 and 1995 cm^{-1} characteristic of an $\text{M}(\text{CO})_2$ metal center. The absence of a band in the region between 1740 and 1770 cm^{-1} ruled out the presence of an unsubstituted fluoroolefin in either product, confirming that these isomeric complexes result from nucleophilic attack at both olefins of 9 rather than at a single olefin. The ^1H NMR spectrum of the mixture exhibited two singlets at 5.02 and 5.05 ppm, of integrated ratio 1:1, assigned to the cyclopentadienyl ring protons of each complex. Six resonances of equal intensity were observed in the ^{19}F NMR spectrum of the mixture, confirming that the ratio of 20:21 produced was 1:1. A pure sample of each complex was obtained by a combination of selective recrystallization and column chromatography. Unfortunately it was not possible to assign a set of ^{19}F NMR signals unambiguously to a specific complex. However, as shown in Table III, the presence of the high-field ^{19}F resonances characteristic of bridgehead fluorines confirmed that the tricyclic ligand remained intact, and the absence of any resonances that could be assigned to fluorines bound to an unsubstituted olefinic carbon was also consistent with the infrared spectral data.

Partial disubstitution was also observed when the reaction of $\text{M}^+[\text{Fe}(\eta^5\text{-C}_5\text{H}_5)(\text{CO})_2]^-$ ($\text{M} = \text{Na}, \text{K}$) with OFCOT was repeated on a larger scale at -78°C followed by warming the solution to room temperature. The equilibrium mixture of 17 and 18 was obtained, together with the disubstituted complex 22. Complex 22 was formed in



higher yields when the reaction was carried out at room temperature. The reaction of 1 equiv of $\text{K}^+[\text{Fe}(\eta^5\text{-C}_5\text{H}_5)(\text{CO})_2]^-$ with 17 also yielded 22. However, under identical conditions, the weaker nucleophiles $\text{Na}^+[\text{M}(\text{CO})_5]$ ($\text{M} = \text{Mn}, \text{Re}$)²⁵ did not react with their respective monosubstituted complexes 7 and 16 to give any identifiable analogues of 22.

The solution infrared spectrum of 22 exhibited two bands in the metal carbonyl region at 2037 and 1989 cm^{-1} characteristic of an $\text{M}(\text{CO})_2$ metal center. The ^1H NMR spectrum displayed only one cyclopentadienyl resonance at δ 4.92 ppm, and the ^{19}F NMR spectrum exhibited three equal-intensity resonances at δ 76.7, 100.6, and 137.1 ppm. These NMR characteristics did not allow a choice to be made between the five possible disubstituted isomers (1,2;

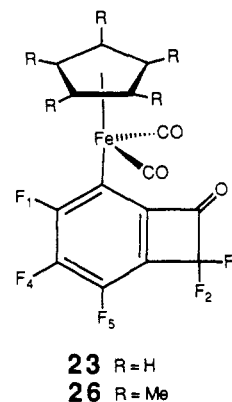
Table IV. Comparison of the ^{19}F NMR Chemical Shift Data for 23, 26, and Two Cobalt Relatives^a ($[[\text{M}](\text{C}_8\text{F}_7)]$)

	[M]	F ₁	F ₂	F ₃	F ₄	F ₅
23	FeCp(CO) ₂	95.0	97.9	97.9	142.6	145.6
26	FeCp*(CO) ₂ ^{b,c}	96.1	98.5	98.5	143.3	146.7
	Co(CO) ₃ (PMe ₂ Ph) ^d	94.5	98.2	98.2	142.0	143.9
	Co(CO) ₃ (PMePh) ₂ ^d	95.6	98.2	98.2	142.0	144.0

^a Shifts quoted in ppm upfield of internal CFCl_3 . ^b Summary of ^{19}F NMR coupling constants (Hz) for 26: $J_{1,4} = 24$; $J_{1,5} = 9$; $J_{4,5} = 20$. Individual J_{FF} couplings for F₂, F₃ with F₁, F₄, or F₅ are <3 Hz. ^c Cp* = pentamethylcyclopentadienyl. ^d While the spectra of these cobalt analogues are included here for completeness and convenience, their actual syntheses are described in the following paper in this issue.

1,4; 1,5; 1,6; 1,8) that possess a plane of symmetry or a 2-fold rotation axis. A single-crystal X-ray diffraction study (see below) unambiguously defined the structure as the 1,5-isomer shown for 22.

Column chromatography of the product mixture from this reaction on Florisil afforded pure samples of 17, 22, and another complex, 23, which was not present in the mixture prior to chromatography. The solution infrared



spectrum of 23 displayed two bands in the metal carbonyl region at 2043 and 2001 cm^{-1} and a band at 1790 cm^{-1} that appeared to be due to a ketone. The ^1H NMR spectrum of 23 exhibited a single cyclopentadienyl resonance at δ 4.0 ppm assigned to the cyclopentadienyl ring protons, and the ^{19}F NMR spectrum of 23 contained four resonances of relative intensity 1:2:1:1 (Table IV). These data are consistent with structure 23, and confirmation has been provided by a crystallographic study to be reported elsewhere.²⁶ The mechanism of formation of 23 remains a mystery, but it clearly arises from interaction of 17 (or 18) with the chromatography support. NMR data for some cobalt analogues are also included in Table IV.²⁷

The reactivity of the pentamethylcyclopentadienyl analogue $\text{K}^+[\text{Fe}(\eta^5\text{-C}_5\text{Me}_5)(\text{CO})_2]^-$ with OFCOT mirrored that of its cyclopentadienyl analogue, affording an equilibrium mixture of 24 and 25. Chromatography of the

(26) Davis, R. E. Unpublished results.

(27) The syntheses of the cobalt analogues are reported in: Hughes, R. P.; Doig, S. J.; Hemond, R. C.; Smith, W. L.; Davis, R. E.; Gadol, S. M.; Holland, K. D. *Organometallics*, following paper in this issue.

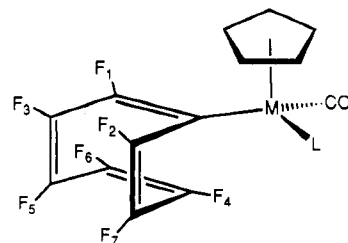
reaction residue on Florisil produced some **26**. The tub conformation of the perfluorinated ligand in **24** was confirmed by a single-crystal X-ray diffraction study (see below).

Similarly, the reaction of $\text{Na}^+[\text{Ru}(\eta^5\text{-C}_5\text{H}_5)(\text{CO})_2]^-$ with OFCOT afforded the monosubstituted complexes **27** (and **28**). Isolation of these complexes did not require column chromatography, and there was no observation of a ruthenium complex analogous to **23** or **26**.

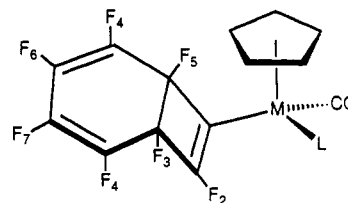
The reactions of a variety of cobalt carbonyl anions with OFCOT yield dinuclear complexes containing the μ -hexafluorocyclooctatrienyl ligand, as well as analogues of the mononuclear heptafluorocyclooctatetraenyl complexes reported in this paper. While full details of the synthesis of these complexes are provided in the following paper, NMR data for (heptafluorocyclooctatetraenyl)cobalt complexes, and their bicyclic valence isomers, are included for comparative purposes in Tables I and II.

Synthesis and Spectroscopic Studies of $[\text{M}(\eta^5\text{-C}_5\text{H}_5)(\eta^1\text{-C}_8\text{F}_7)(\text{CO})\text{L}]$ ($\text{M} = \text{Fe}$, $\text{L} = \text{CO}$, PPh_3 , AsPh_3 ; $\text{M} = \text{Ru}$, $\text{L} = \text{CO}$) Complexes. The observation of the temperature-independent ^{19}F NMR spectra of **7** and **16** indicated that the isodynamic BS process is slow on the NMR time scale but gave no insight into the isodynamic RI process. The presence of two diastereotopic CO ligands on **17** presented an opportunity to evaluate the barrier to the RI process. The temperature independence of the ^{19}F NMR spectrum of **17** up to 60 °C ruled out the possibility of an isodynamic BS process, consistent with the result obtained for **7** and **16**. In addition, the ^{19}F NMR spectrum of the ruthenium analogue **27** was also shown to be independent of temperature up to 100 °C. However, at 80 °C the $^{13}\text{C}\{^{19}\text{F}\}$ NMR spectrum of **17** still displayed eight cyclooctatetraene ring carbon resonances as well as two resonances at δ 212.53 and 212.45 ppm due to diastereotopic CO ligands. The observation of the two CO signals indicates that the RI process must also be slow on the NMR time scale. This absence of coalescence in the $^{13}\text{C}\{^{19}\text{F}\}$ NMR spectrum at 80 °C allowed a minimum value of $\Delta G^*_{\text{RI}} \geq 18.9 \text{ kcal mol}^{-1}$ to be calculated. However, the actual value for ΔG^*_{RI} is possibly much greater, since the equation used to obtain ΔG^*_{RI} is dependent upon the line separation between the exchangeable nuclei, which in this case is small (7 Hz). Clearly, a sufficiently high barrier to RI would result in epimerization of the cyclooctatetraene ring being sufficiently slow so as to allow separation of diastereoisomers. As discussed in the Introduction, substitution of one CO on **17** with a phosphine or arsine ligand would afford a complex with an asymmetric metal center. When this is coupled with the conformational asymmetry of the monosubstituted cyclooctatetraene ring, two diastereoisomeric pairs with different physical and spectroscopic properties should be formed. As shown in Scheme I, the RI process must epimerize the conformationally asymmetric ring and interconvert diastereoisomers, a process that could be monitored with use of NMR spectroscopy.

Irradiation of a hexane solution containing **17** and triphenylphosphine afforded **29** as a 1:1 mixture of diastereoisomers, as indicated by two equal-intensity sets of seven resonances in the ^{19}F NMR spectrum. An analogous reaction with triphenylarsine afforded **30**, as a 2:1 diastereoisomeric mixture. A single recrystallization of each mixture afforded pure samples of a single diastereoisomer (compound numbers corresponding to pure diastereoisomers will be given arbitrary suffixes **a** or **b** to facilitate discussion, though absolute configurations are unknown). Small peaks due to the corresponding bicyclic valence isomers

**29** L = PPh₃**30** L = AsPh₃

31 and **32** were observed in the NMR spectra of both pure

**31** L = PPh₃**32** L = AsPh₃

and mixed diastereoisomers. Clearly the stability of these pure diastereoisomers at room temperature indicates that RI is not just slow on the NMR time scale but is a chemically slow event.

A purified triphenylarsine diastereoisomer was used in a kinetic experiment, in which **30a** and a known quantity of trifluorotoluene (as an internal standard) were dissolved in benzene-*d*₆ in a medium-walled NMR tube and the tube was sealed under vacuum. The integrated area of the CF₃ resonance was set at 1.00 and was compared to the area of the two lowest field signals in **30a**. Both low-field signals were used, so as to obtain two values for the RI rate that could then be averaged. The sample was warmed to a carefully calibrated temperature in a bath. At various time intervals the sample was removed and quenched at -196 °C, and a ^{19}F NMR spectrum was then taken at room temperature (at which temperature the rate of RI is slow). The relative integration of each of the two signals in the original diastereoisomer **30a** was compared with the corresponding signal in the new diastereoisomer **30b**. A plot of $\ln \left(\frac{[A]_t - [A]_\infty}{[A]_0 - [A]_\infty} \right)$ (where $[A]_t$ = the relative integration of the ^{19}F NMR resonance in **30a** at the time *t* (min) when the reaction was quenched) versus time afforded the rate constant for the conversion of **30a** to **30b**. This experiment was carried out at four different temperatures and allowed the following kinetic parameters to be calculated for the process by which **30a** is transformed to **30b**: $E_a = 23.0 (\pm 0.9) \text{ kcal mol}^{-1}$, $\ln A = 26.1 (\pm 1.4)$, $\Delta G^* = 24.4 (\pm 0.3) \text{ kcal mol}^{-1}$, $\Delta H^* = 22.4 (\pm 0.9) \text{ kcal mol}^{-1}$, and $\Delta S^* = -6.6 (\pm 1.8) \text{ eu}$. As a control experiment **30a** was heated under an atmosphere of ^{13}CO . Labeled CO was incorporated into both **30a** and **30b**, indicating that diastereomer interconversion may not result from inversion of the conformationally asymmetric fluorinated ring. Epimerization at the metal center via a CO dissociation/recombination reaction or by associative substitution of CO via a Cp ring slippage mechanism cannot be ruled out by these data. We cannot distinguish whether the kinetic parameters obtained above are appropriate for either a pure epimerization reaction at the metal or a combination epimerization plus RI mechanism; clearly, if epimerization at the metal center is the sole mechanism interconverting **30a** and **30b**, these kinetic parameters represent *minimum* values for RI of the eight-membered ring.

Table V. Crystallographic Summary for Complexes 17, 24, 22, and 13

	17	24	22	13
A. Crystal Data (-110 °C) ^a				
<i>a</i> , Å	21.390 (5)	15.307 (4)	11.317 (2)	12.131 (2)
<i>b</i> , Å	7.507 (1)	13.952 (3)	11.458 (2)	8.491 (1)
<i>c</i> , Å	18.767 (5)	9.058 (2)	8.006 (2)	14.892 (2)
α , deg	90	90	99.13 (1)	90
β , deg	108.63 (2)	92.01 (2)	91.04 (1)	112.05 (2)
γ , deg	90	90	93.63 (1)	90
<i>V</i> , Å ³	2855.5 (11)	1933.1 (8)	1022.5 (4)	1421.8 (4)
no. of rflns for cell data	45	45	60	45
2θ range for cell data, deg	17.5–24.1	14.5–20.7	24.0–29.7	24.1–26.7
<i>d</i> _{calcd} , g cm ⁻³ (-110 °C)	1.889	1.636	1.832	1.981
<i>d</i> _{measd} , g cm ⁻³ (21 °C)	1.900	1.627		
chem formula	C ₁₅ H ₅ O ₂ F ₇ Fe	C ₂₀ H ₁₅ O ₂ F ₇ Fe	C ₂₂ H ₁₀ O ₄ F ₆ Fe ₂	C ₁₃ O ₅ F ₇ Mn
fw	406.06	476.19	564.00	424.07
cryst syst	monoclinic	monoclinic	triclinic	monoclinic
space group, <i>Z</i>	<i>C</i> 2/ <i>c</i> (No. 15), 8	<i>P</i> 2 ₁ / <i>n</i> (No. 14), 4	<i>P</i> 1 (No. 2), 2	<i>P</i> 2 ₁ / <i>c</i> (No. 14), 4
<i>F</i> (000), electrons	1600	960	560	824
B. Data Collection (-110 °C) ^b				
radiation, λ , Å	Mo K α , 0.71069			
mode	ω scan			
scan range	symmetrically over 1.0° about K α _{1,2} max			
bkgd	offset 1.0 and -1.0° in ω from K α _{1,2} max			
scan rate, deg min ⁻¹	3.0–6.0			
2θ range, deg	4.0–55.0	4.0–55.0	4.0–60.0	4.0–60.0
exposure time, h	43.6	57.8	80.1	60.3
stability analysis				
computed <i>s</i> , <i>t</i>	-0.000062, 0.0	0.000087, -0.000002	0.001392, -0.000016	-0.000595, 0.000009
correction range (on <i>l</i>)	1.00–1.01	0.99–1.00	0.97–1.00	0.94–1.00
total no. of rflns measd	3286	4443	6231	4497
data cryst vol, mm ³	0.0083	0.0117	0.0092	
data cryst faces	{001}, {301}, 111, $\bar{1}\bar{1}\bar{1}$	0 $\bar{1}$ 3, 013, $\bar{2}$ 10, $\bar{2}$ 1 $\bar{0}$, $\bar{2}$ 31, $\bar{2}$ 3 $\bar{1}$	{100}, {010}, {001}, { $\bar{1}$ 01}	
abs coeff, μ (Mo K α), cm ⁻¹	11.52	8.89	15.46	10.96
transmissn factor range	0.703–0.856	0.853–0.891	0.688–0.842	
C. Structure Refinement ^c				
ignorance factor, <i>p</i>	0.02	0.02	0.02	0.02
no. of rflns used, $F_o \leq 4\sigma(F_o)$	2660	3612	4495	3422
no. of variables	246	286	289	290
<i>R</i> , <i>R</i> _w	0.053, 0.050	0.036, 0.034	0.052, 0.061	0.046, 0.043
<i>R</i> , <i>R</i> _w for all data	0.072, 0.054	0.055, 0.038	0.081, 0.062	0.066, 0.046
goodness of fit, <i>S</i>	5.49	1.80	2.40	1.90
max shift/esd	1.35 (x for H9)	0.21	0.01	0.01
max peak in diff map, e Å ⁻³	0.58	48	1.04	0.75

^a Unit cell parameters were obtained by least-squares refinement vs the number of reflections shown, in the 2θ range given. Crystal densities for 17 and 24 were measured by flotation in an aqueous ZnCl₂ solution. Densities of the other two crystals were not measured. ^b Syntex P₂ autodiffractometer with a graphite monochromator and a Syntex LT-1 inert-gas (N₂) low-temperature delivery system. Data reduction was carried out as described in: Riley, P. E.; Davis, R. E. *Acta Crystallogr., Sect. B* 1976, 32, 381. Crystal and instrument stability were monitored by remeasurement of four check reflections after every 96 reflections. These data were analyzed as detailed in: Henslee, W. H.; Davis, R. E. *Acta Crystallogr., Sect. B* 1975, 31, 1511. ^c Relevant expressions are as follows: function minimized $\sum w(|F_o| - |F_c|)^2$, where $w = (\sigma|F|)^{-2}$; $R = \sum(|F_o| - |F_c|)/\sum|F_o|$; $R_w = [\sum w(|F_o| - |F_c|)^2/\sum w|F_o|^2]^{1/2}$; $S = [\sum w(|F_o| - |F_c|)^2/(m - n)]^{1/2}$.

We can conclude that heptafluorination of the eight-membered ring in these mononuclear iron complexes raises the barrier to the RI process as compared to that for the hydrocarbon analogues. This discrepancy ($\Delta\Delta G^*_{RI} \geq 7.1$ kcal mol⁻¹) must be attributed solely to the presence of fluorines on the ring and is not unexpected since heptafluorocyclooctatetraene was found to have a larger $E_{a,BS}$ value than the parent COT molecule.²⁴ The difference in the latter system was ascribed to steric buttressing interactions between the slightly larger fluorine substituents in going from the ground-state tub conformation to the planar intermediate, and similar arguments can be made for the organometallic analogues discussed herein.

Solid-State Structures. The solid-state structure of OFCOT has been determined previously,⁵ and selected bond angles and bond lengths are shown in Figure 1a. The eight-membered ring adopts a tub conformation, as found for its hydrocarbon analogue COT.²⁸ The degree of

flattening of the ring is defined by the dihedral angles (α) between the plane formed by two nonadjacent double bonds and the plane formed by one other double bond and the two single bonds adjacent to it: i.e., as α increases, the amount of flattening decreases.⁵ In OFCOT, the dihedral angle α between the planes defined by [C(1),C(2),C(5),C(6)] and [C(2),C(3),C(4),C(5)] is 41.8 (2)°, while α for the planes defined by [C(1),C(2),C(5),C(6)] and [C(6),C(7),C(8),C(1)] is 41.4 (2)°. The averaged C—C, C=C, and C—F bond lengths are 1.475 (3), 1.340 (3), and 1.346 (3) Å, respectively.⁵

Molecular Structure of [Fe(η^5 -C₅H₅)(η^1 -C₈F₇)(CO)₂] (17). A thermal ellipsoid plot of the molecular structure of 17 is shown in Figure 2a. Details of the structure determination are shown in Table V, and selected bond angles and bond lengths are shown in Figure 1b. Fractional atomic coordinates and full listings of bond lengths and angles for all complexes are provided as supplementary material. The coordination geometry around the iron atom can be described as octahedral, if the cyclopentadienyl ligand is considered to occupy three coordination sites and

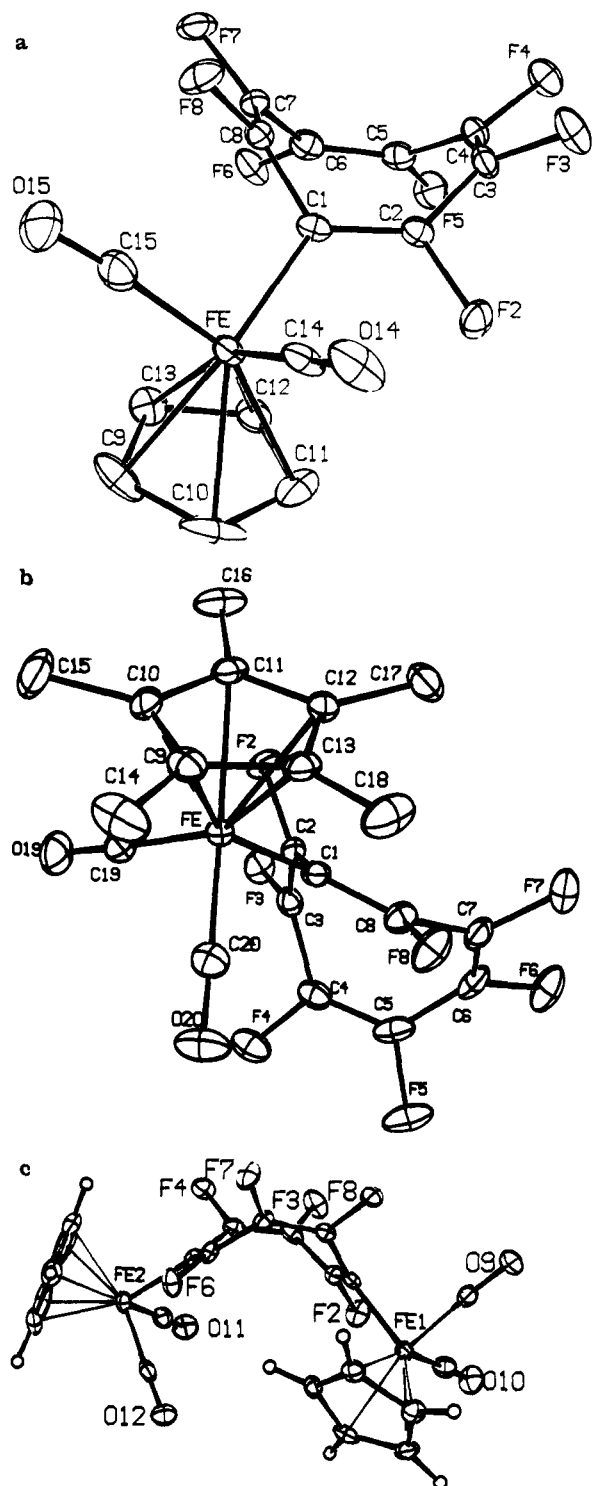


Figure 2. Thermal ellipsoid plots and atomic numbering schemes for (a) complex 17, (b) complex 24, (c) complex 22.

the carbonyl ligands and σ -bound C_8F_7 fragment occupy one site each. The C_8F_7 ligand adopts the expected tub conformation with an α of $42.4(6)^\circ$ for the planes defined by $[C(1), C(2), C(5), C(6)]$ and $[C(6), C(7), C(8), C(1)]$ and $39.6(6)^\circ$ for $[C(1), C(2), C(5), C(6)]$ and $[C(2), C(3), C(4), C(5)]$, as compared to the corresponding angles in OFCOT of $41.8(2)$ and $41.4(2)^\circ$.⁵ The Fe-C σ -bond (sp^2) in 17, $1.977(10)$ Å, is shorter than the corresponding Fe-C σ -bond (sp^2) length of $2.11(1)$ Å to the phenyl ring in $[Fe(\eta^5-C_5H_5)(\eta^1-C_6H_5)(CO)(PPh_3)]^{29}$ but longer than that to the

pentafluorocyclobutenyl ring ($1.936(9)$ Å) in $[Fe(\eta^5-C_5H_5)(\eta^1-C_4F_5)(CO)_2]^{19p}$.

The individual C-C and C-F bond lengths in 17 are not significantly (>3 esd) different from the corresponding bonds observed for OFCOT (Figure 1).⁵ The $C(2)-C(1)-C(8)$ bond angle of $118.7(6)^\circ$ is significantly smaller than the corresponding angles in OFCOT, which range between $126.3(2)$ and $127.4(2)^\circ$, while the adjacent $C(1)-C(2)-C(3)$ and $C(1)-C(8)-C(7)$ bond angles of $131.1(6)$ and $129.3(7)^\circ$, respectively, are larger than the other C-C-C bond angles in 17 or OFCOT. This general phenomenon of contraction of the bond angle at the ligated carbon atom, and expansion of the adjacent angles, has been observed in a variety of other systems, including the pentafluorocyclobutenyl complex $[Fe(\eta^5-C_5H_5)(\eta^1-C_4F_5)(CO)_2]^{19p}$ and several pentafluorophenyl complexes.³⁰

As observed in the phenyl complex $[Fe(\eta^5-C_5H_5)(\eta^1-C_6H_5)(CO)(PPh_3)]^{29}$ and the pentafluorocyclobutenyl complex $[Fe(\eta^5-C_5H_5)(\eta^1-C_4F_5)(CO)_2]^{19p}$ steric hindrance between the metal carbonyl ligands and the tub-shaped C_8F_7 ring in 17 causes the Fe-C σ -bond to deviate by $6.9(10)^\circ$ from the plane composed of $[Fe, C(1), C(2), F(2)]$. In each of the other planes composed of F-C=C-F fragments, the deviation of the individual C-F bonds is insignificant. This type of steric interaction has an effect on the conformation of the fluorinated ring in 17; e.g., the $C(2)-C(1)-C(8)$ bond angle is smaller, while the adjacent $C(1)-C(2)-C(3)$ and $C(1)-C(8)-C(7)$ bond angles are larger than the other C-C-C bond angles in 17. Therefore, it appears that as the iron fragment pushes away from the C_8F_7 ring the perfluorinated ring undergoes small conformational adjustments to minimize any resulting ring strain.

Molecular Structure of $[Fe(\eta^5-C_5Me_5)(\eta^1-C_8F_7)(CO)_2]$ (24). A plot of the molecular structure of 24 is shown in Figure 2b. Details of the structure determination are shown in Table V, and selected bond angles and bond lengths are shown in Figure 1c. As observed in 17, the iron atom is in an octahedral environment with the C_8F_7 ligand in the tub conformation. The values for α of $41.0(2)^\circ$ $[C(1), C(2), C(3), C(8)]$ and $[C(3), C(4), C(7), C(8)]$ and $40.7(2)^\circ$ $[C(4), C(5), C(6), C(7)]$ and $[C(3), C(4), C(7), C(8)]$ are similar to the corresponding values of $42.4(6)$ and $39.6(6)^\circ$ in 17. The individual bond lengths and angles in 24 are not significantly different from the corresponding values in 17 (Figure 1). The Fe-C σ -bond deviates from the plane composed of $[Fe, C(1), C(2), F(2)]$ by $4.7(3)^\circ$, which is only marginally smaller than the value of $6.9(10)^\circ$ observed in 17. Thus, the bulky C_5Me_5 ligand, which is on the side of the metal away from the fluorinated ring, has little effect on the magnitude of the steric interaction between the C_8F_7 ring and the metal fragment.

Molecular Structure of $[(Fe(\eta^5-C_5H_5)(CO)_2)_2(\mu_2-C_8F_6)]$ (22). A thermal ellipsoid plot of the molecular structure of 22 is shown in Figure 2c. Details of the structure determination are shown in Table V, and selected bond angles and bond lengths are shown in Figure 1d. The two dihedral angles (α) and most of the bond lengths and angles in 22 are not significantly different from those in 17. Although all of the C-F bond lengths in 22 are significantly longer than the individual C-F bond lengths in OFCOT,⁵ only the $C(4)-F(4)$ ($1.368(5)$ Å) and $C(8)-F(8)$ ($1.370(5)$ Å) bond lengths are significantly different from the corresponding bond length of $1.343(9)$ Å for $C(8)-F(8)$ in 17. The $C(2)-C(1)-C(8)$ bond angle ($115.8(4)^\circ$) and the $C(4)-C(5)-C(6)$ bond angle ($116.6(4)^\circ$) are even smaller

(29) Avoyan, R. L.; Chapovskii, Yu. A.; Struchkov, Yu. T. *J. Struct. Chem. (Engl. Transl.)* 1966, 7, 538.

(30) Jones, P. G. *J. Organomet. Chem.* 1988, 345, 405.

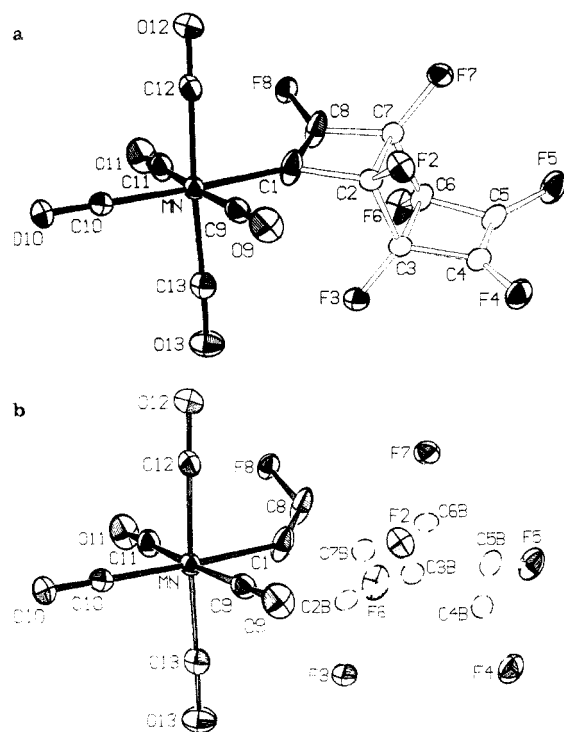


Figure 3. Thermal ellipsoid plots and atomic numbering schemes for complex 13: (a) major occupancy sites; (b) minor occupancy sites.

than the corresponding bond angle ($118.7(6)^\circ$) in 17. The Fe(1)–C(1) σ -bond deviates from the plane composed of [Fe(1), C(1), C(2), F(2)] by $9.0(7)^\circ$, as compared to $6.9(10)^\circ$ in 17. Presumably due to the presence of the bulky cyclopentadienyl group on Fe(1), the second iron fragment orientates itself differently from the first with respect to the C_8F_6 ligand, which results in only a minor deviation ($0.3(6)^\circ$) of the Fe(2)–C(5) σ -bond from the plane composed of [Fe(2), C(5), C(6), F(6)].

Molecular Structure of [Mn(η^1 -C₈F₇)(CO)₅] (13). Details of the structure determination are shown in Table V. As a result of the disorder of the tricyclic carbon skeleton found in the unit cell, there are major- and minor-occupancy structures for 13. Plots of both structures of 13 are shown in Figure 3. Selected bond angles and bond lengths for the major structure (Figure 3a) are shown in Figure 4. The coordination geometry around the manganese atom is octahedral, and the overall anti configuration of the tricyclic ring is unchanged from that of the unsubstituted fluorocarbon 9. The overall geometry of the [Mn(CO)₅] fragment is not significantly different from that observed in [Mn₂(CO)₁₀],³¹ and the Mn–C(1) σ -bond length of $2.031(3) \text{ \AA}$ is not significantly different from the corresponding bond length ($1.95(3) \text{ \AA}$) observed in the related complex (*cis*-1,2-difluorovinyl)penta-carbonylmanganese.³²

Experimental Section

General Considerations. Infrared spectra were recorded on a Perkin-Elmer 257 or 599 dispersive infrared spectrophotometer, calibrated against the 1601 cm^{-1} peak of polystyrene, or on a Bio-Rad Digilab FTS-40 Fourier transform infrared spectrophotometer. ¹H NMR spectra (300 MHz) and ¹³C{¹H} and ¹³C{¹⁹F} spectra (75 MHz) were recorded on a Varian Associates XL-300 spectrometer at 25°C unless otherwise noted. ¹⁹F NMR spectra were recorded on a JEOL FX60Q spectrometer (56.2 MHz) or

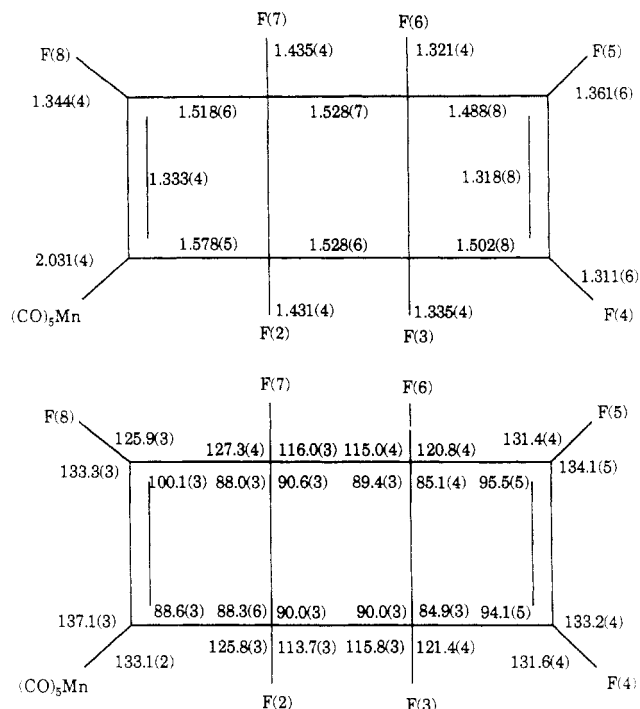


Figure 4. Bond lengths (\AA) and angles (deg) for the fluorinated ring in complex 13, involving only the ordered atoms and the major-site atoms. Values involving the minor-site atoms are available in the supplementary material. Values for C–C lengths and C–C–C angles appear inside the ring. Values for C–F lengths and C–C–F angles appear outside the ring.

on a Varian Associates XL-300 spectrometer at 25°C unless otherwise noted. All ¹⁹F NMR shifts were recorded as ppm upfield from the internal standard CFC1₃. All ¹H and ¹³C shifts were recorded as ppm downfield from tetramethylsilane. All variable-temperature NMR spectra were taken on a Varian Associates XL-300 spectrometer. The probe was calibrated at various temperatures by using samples of methanol (low temperature)³³ and ethylene glycol (high temperature).³⁴ Melting points were determined with an Electrothermal capillary melting point apparatus and are uncorrected. Positive ion fast atom bombardment (FAB) mass spectra were recorded at the Johns Hopkins School of Medicine Middle Atlantic Mass Spectrometry Laboratory. Microanalyses were done at Atlantic Microlab, Inc., Atlanta, GA, or Spang Microanalytical Laboratory, Eagle Harbor, MI.

All solvents were dinitrogen-saturated and distilled over a variety of drying agents. Benzene and tetrahydrofuran were dried over potassium, toluene was dried over sodium, hexane, petroleum ether, and diethyl ether were dried over sodium–potassium alloy, and methylene chloride was dried over P₂O₁₀. All reactions were run in oven-dried glassware with use of conventional Schlenk techniques, under an atmosphere of dinitrogen that was deoxygenated over BASF catalyst and dried with Aquasorb or in a Vacuum Atmospheres Dry Box equipped with an HE-492 gas purification system. Column chromatography was done under dinitrogen in jacketed columns with dry, N₂-saturated chromatography supports and solvents. All deuterated solvents were dried over P₄O₁₀ and degassed prior to use.

Silica gel (Davisol 62, activity III) was obtained from Davison Chemical, Inc. Alumina (activity III) was obtained from ICN Pharmaceuticals, Inc. Florisil was obtained from Fisher Scientific Co. Triphenylphosphine and triphenylarsine were obtained from Aldrich Chemical Co. and used as supplied. Hexafluorobenzene was obtained from Fairfield Chemical Co. 1,2-Difluoro-1,2-dichloroethylene was obtained from PCR Research Chemicals, Gainesville, FL. Octafluorocyclooctatetraene (OFCOT; 1) and anti-octafluorotricyclo[4.2.0.0^{2,5}]octa-3,7-diene (9) were prepared according to the method of Lemal.⁴ K⁺[Fe(η^5 -C₅H₅)(CO)₂]^{−35} and

(31) Churchill, M. R.; Amoh, K. N.; Wasserman, H. J. *Inorg. Chem.* 1981, 20, 1609.

(32) Einstein, F. W. B.; Luth, H.; Trotter, J. J. *Chem. Soc. A* 1967, 89.

(33) Van-Geet, A. L. *Anal. Chem.* 1968, 40, 2227.

(34) Piccini-Leopardi, C.; Fabre, O.; Reisse, J. *Org. Chem. Magn. Reson.* 1976, 8, 233.

$\text{Li}^+[\text{Fe}(\eta^5\text{-C}_5\text{H}_5)(\text{CO})_2]^-$ were prepared by literature procedures. A sample of $[\text{Ru}(\eta^5\text{-C}_5\text{H}_5)(\text{CO})_2]_2$ was generously donated by Professor John Hubbard at the University of Vermont. Samples of $[\text{Re}_2(\text{CO})_{10}]$ and $[\text{Mn}_2(\text{CO})_{10}]$ were purchased from Pressure Chemical Co.

Reaction of $\text{Na}^+[\text{Mn}(\text{CO})_5]^-$ with OFCOT. $[\text{Mn}_2(\text{CO})_{10}]$ (0.50 g, 1.3 mmol) was dissolved in THF (30 mL) and added to a 0.5% Na/Hg amalgam. The yellow solution became gray/green over a 3-h period and was then filtered through Celite. The clear yellow solution was then added over a 30-min period at room temperature to a stirred THF (15 mL) solution of OFCOT (1.24 g, 5.0 mmol). After 96 h the reaction solvent was removed under reduced pressure and the residue was chromatographed on Florisil. Elution with hexane (total amount of solvent 200 mL) gave a pale yellow band from which $[\text{Mn}_2(\text{CO})_{10}]$ was obtained. Elution with CH_2Cl_2 /hexane (50%/50%; total amount of solvent 150 mL) produced a pale yellow band. Removal of the solvent under reduced pressure followed by crystallization from CH_2Cl_2 /hexane at -20°C afforded the white solid **7** (0.54 g, 50%), mp $77\text{--}78^\circ\text{C}$. ^{19}F NMR (CDCl_3): δ 67.1 (m, F_1), 93.9 (m, F_2), 119.9 (m, F_3), 125.7 (m, F_4), 127.8 (m, F_5), 130.1 (m, F_6), 141.3 (m, F_7); a complete analysis of the coupling constants for an isostructural complex (**27**) appears below, and inspection reveals a similar coupling pattern for **7**. IR (hexane): $\nu_{\text{CO}} = 2126, 2170, 2037, 2013, 1970\text{ cm}^{-1}$. Anal. Calcd for $\text{C}_{13}\text{F}_7\text{MnO}_5$: C, 36.80. Found: C, 36.88. There is an equilibrium in solution between **7** and its bicyclic valence isomer **12** (**12**: ^{19}F NMR (CDCl_3) δ 93.2 (m, F_2), 144.3 (m, F_3), 150.8 (m, F_4), 151.1 (m, F_5), 155.3 (m, F_6), 158.7 (m, F_7), 161.9 (m, F_8); the assignment of the fluorine signals in **12** was made by a comparison with the coupling constants for the isostructural compound **11**²⁴).

Preparation of ((3 η)-anti-Heptafluorotricyclo[4.2.0.0^{2,5}]-octa-1,5-dienyl)pentacarbonylmanganese(I) (13**).** To a stirred solution of anti-octafluorotricyclo[4.2.0.0^{2,5}]octa-3,7-diene (**9**; 0.61 g, 2.45 mmol) in THF (5 mL) was added $\text{Na}^+[\text{Mn}(\text{CO})_5]^-$ (0.71 g, 3.1 mmol) as a solid, at room temperature. The solution was stirred for 170 h and the solvent removed under reduced pressure. The residue was subjected to column chromatography on silica gel at 8°C . Elution with hexane (total amount of solvent 150 mL) gave a bright yellow band from which a pale yellow solid was obtained. Sublimation of this solid (0.1 Torr, 40°C , 4 h) afforded white crystals of **13** suitable for X-ray diffraction studies (0.20 g, 20%); mp $59\text{--}61^\circ\text{C}$. ^{19}F NMR (CDCl_3): δ 98.6 (m, F_1), 120.2 (m, F_2), 120.4 (m, F_3), 171.2 (m, F_4), 180.0 (m, F_5), 185.9 (m, F_6), 188.2 (m, F_7); a complete analysis of the coupling constants for an isostructural complex (**19**) appears below, and inspection reveals a similar coupling pattern for **13**. IR (hexane): $\nu_{\text{CO}} = 2130, 2075, 2040, 2015, 1985\text{ cm}^{-1}$; $\nu_{\text{FC}=\text{CF}} = 1755\text{ cm}^{-1}$; $\nu_{\text{Mn}=\text{CF}} = 1609\text{ cm}^{-1}$. Anal. Calcd for $\text{C}_{13}\text{F}_7\text{MnO}_5$: C, 36.80. Found: C, 36.69. The elemental composition was also confirmed by an X-ray diffraction study.

Reaction of $\text{Na}^+[\text{Re}(\text{CO})_5]^-$ with OFCOT. A sample of $[\text{Re}_2(\text{CO})_{10}]$ (0.51 g, 0.78 mmol) was dissolved in THF (20 mL) to afford a colorless solution that was then added to a 0.5% Na/Hg amalgam at 0°C over a 5-min period. After 3 h the gray/green solution was filtered through Celite and the clear orange filtrate added to a room-temperature stirred THF (15 mL) solution of OFCOT (0.73 g, 2.9 mmol). The orange solution was stirred for 96 h and gradually became golden yellow. The reaction solvent was removed under reduced pressure and the residue subjected to column chromatography on Florisil. Elution with hexane (total amount of solvent 140 mL) afforded a colorless band from which $[\text{Re}_2(\text{CO})_{10}]$ was obtained. Elution with CH_2Cl_2 /hexane (50%/50%; total amount of solvent 150 mL) gave a colorless band from which a white solid was obtained. Crystallization from CH_2Cl_2 /hexane at -30°C yielded white crystals of **16** (0.22 g, 28%), mp $100\text{--}101^\circ\text{C}$. ^{19}F NMR (CDCl_3): δ 65.1 (m, F_1), 93.6 (m, F_2), 120.5 (m, F_3), 125.2 (m, F_4), 127.8 (m, F_5), 129.7 (m, F_6), 142.2 (m, F_7); a complete analysis of the coupling constants for an isostructural complex (**27**) appears below, and inspection reveals a similar coupling pattern for **16**. $^{13}\text{C}\{^{19}\text{F}\}$ NMR (CDCl_3 , 75 MHz): δ 115.95 ($=\text{C}-\text{Re}$), 128.30, 136.56, 137.49, 138.48, 139.80, 150.64,

152.94 (all $=\text{C}-\text{F}$), 179.37 (CO_{trans}), 179.68 (CO_{cis}). IR (hexane): $\nu_{\text{CO}} = 2142, 2076, 2035, 2005, 1972\text{ cm}^{-1}$. Anal. Calcd for $\text{C}_{13}\text{F}_7\text{O}_5\text{Re}$: C, 28.11. Found: C, 28.16.

Reaction of $\text{K}^+[\text{Fe}(\eta^5\text{-C}_5\text{H}_5)(\text{CO})_2]^-$ with OFCOT. Formation ($\eta^5\text{-Cyclopentadienyl})(\eta^1\text{-heptafluorocyclooctatetraenyl})\text{dicarbonyliron(II)}$ (17**).** To a stirred THF (15 mL) solution of OFCOT (0.98 g, 3.9 mmol) at -78°C was added a bright orange -78°C THF (60 mL) solution of $\text{K}^+[\text{Fe}(\eta^5\text{-C}_5\text{H}_5)(\text{CO})_2]^-$ (0.75 g, 3.5 mmol) over a 30-min period. The deep black/red solution was stirred at -78°C for 12 h. After the anion was quenched with air, the solution was warmed to room temperature and filtered through Celite. The volume of the clear yellow filtrate was reduced to ~ 5 mL and hexane added to precipitate out a yellow solid. Crystallization of this solid twice from CH_2Cl_2 /hexane at -20°C afforded dull yellow crystals of **17** (1.03 g, 73%), mp $98\text{--}99^\circ\text{C}$. ^{19}F NMR (CDCl_3): δ 74.5 (m, F_1), 93.8 (m, F_2), 119.0 (m, F_3), 124.8 (m, F_4), 129.0 (m, F_5), 130.8 (m, F_6), 140.3 (m, F_7); a complete analysis of the coupling constants for an isostructural complex (**27**) appears below, and inspection reveals a similar coupling pattern for **17**. ^1H NMR (CDCl_3): δ 4.98 (s, C_5H_5). $^{13}\text{C}\{^{19}\text{F}\}$ NMR (CDCl_3 , 50 MHz): δ 85.51 (d, $J_{\text{CH}} = 181\text{ Hz}$, C_5H_5), 126.07 ($=\text{C}-\text{Fe}$), 127.60, 136.30, 137.73, 138.84, 140.24, 149.81, 152.87 (all $=\text{C}-\text{F}$), 212.45 (CO), 212.53 (CO). IR (hexane): $\nu_{\text{CO}} = 2047, 1997\text{ cm}^{-1}$. MS: m/e 406 (M^+). Anal. Calcd for $\text{C}_{15}\text{H}_5\text{F}_7\text{FeO}_2$: C, 44.37; H, 1.24. Found: C, 44.50; H, 1.27. Elemental composition was confirmed by an X-ray diffraction study. There is an equilibrium in solution between **17** and its bicyclic valence isomer **18** (**18**: ^{19}F NMR (CDCl_3) δ 98.1 (m, F_2), 144.3 (m, F_3), 151.0 (m, F_4), 155.2 (m, F_5), 159.0 (m, F_6), 162.8 (m, F_7); the assignment of the fluorine signals in **18** was made by a comparison with the coupling constants for the isostructural compound **11**²⁴).

Formation of ($\eta^5\text{-Cyclopentadienyl})(\eta^1\text{-heptafluorocyclooctatetraenyl})\text{dicarbonyliron(II)}$ (17**), ($\mu_2\text{-}(1\eta,5\eta)\text{-Hexafluorocyclooctatetraenediyl})\text{bis}[(\eta^5\text{-cyclopentadienyl})\text{dicarbonyliron(II)}]$ (**22**), and ($\eta^5\text{-Cyclopentadienyl})(5\eta\text{-}7\text{-oxopentafluorobicyclo[4.2.0]octa-1,3,5-trienyl})\text{dicarbonyliron(II)}$ (**23**).** To a stirred orange solution of $\text{K}^+[\text{Fe}(\eta^5\text{-C}_5\text{H}_5)(\text{CO})_2]^-$ (1.5 g, 6.9 mmol) in THF (35 mL) at -78°C was added a -78°C solution of OFCOT (1.75 g, 6.9 mmol) in THF (10 mL). The deep red/black solution was stirred at -78°C for 5 min and then warmed to room temperature, where it was stirred for 1 h. The reaction solvent was removed under reduced pressure and the residue subjected to column chromatography on Florisil. Elution with CH_2Cl_2 /hexane (10%/90%; total amount of solvent 200 mL) produced a bright orange/yellow band. Removal of the solvent under reduced pressure followed by crystallization from CH_2Cl_2 /hexane afforded **17** and its bicyclic valence isomer **18** (1.1 g, 39%). Elution with CH_2Cl_2 /Et₂O (50%/50%; total amount of solvent 100 mL) gave a yellow band from which a deep red/yellow oil was obtained. Chromatography of the oil on Florisil afforded a yellow band upon elution with CH_2Cl_2 /hexane (50%/50%; total amount of solvent 100 mL). Removal of the solvent under reduced pressure followed by crystallization from CH_2Cl_2 /hexane afforded **23** (0.18 g, 7%), mp $127\text{--}129^\circ\text{C}$. ^{19}F NMR (CDCl_3): δ 95.0 (m, F_1), 97.9 (m, F_2), 97.9 (m, F_3), 142.6 (m, F_4), 145.6 (m, F_5); a complete analysis of the coupling constants for the isostructural complex **26** appears below, and inspection reveals a similar coupling pattern for **23**. ^1H NMR (C_6D_6): δ 4.0 (C_5H_5). IR (hexane): $\nu_{\text{Fe}-\text{CO}} = 2043, 2001\text{ cm}^{-1}$; $\nu_{\text{CO}} = 1789\text{ cm}^{-1}$. MS: m/e 556 ($\text{M}^+ - \text{CO}$). Anal. Calcd for $\text{C}_{15}\text{H}_5\text{F}_5\text{FeO}_3$: C, 46.89; H, 1.30. Found: C, 47.08; H, 1.61. The elemental composition was confirmed by an X-ray diffraction study. Elution with CH_2Cl_2 (total amount of solvent 150 mL) from the original column produced a yellow band. Removal of the solvent under reduced pressure followed by crystallization from CH_2Cl_2 /hexane afforded yellow crystals of **22** (0.03 g, 1%), mp $158\text{--}160^\circ\text{C}$ dec. ^{19}F NMR (CDCl_3): δ 76.7 (m, 2 F), 100.6 (m, 2 F), 137.1 (m, 2 F). IR (CH_2Cl_2): $\nu_{\text{CO}} = 2037, 1989\text{ cm}^{-1}$. MS: m/e 564 (M^+). Anal. Calcd for $\text{C}_{22}\text{H}_{10}\text{F}_6\text{Fe}_2\text{O}_4$: C, 46.83; H, 1.77. Found: C, 46.84; H, 1.69. The elemental composition was confirmed by an X-ray diffraction study.

Reaction of $[\text{Fe}(\eta^5\text{-C}_5\text{H}_5)(\eta^1\text{-C}_8\text{F}_7)(\text{CO})_2]$ (17**) with $\text{K}^+[\text{Fe}(\eta^5\text{-C}_5\text{H}_5)(\text{CO})_2]^-$.** To a stirred solution of $\text{K}^+[\text{Fe}(\eta^5\text{-C}_5\text{H}_5)(\text{CO})_2]^-$ (0.25 g, 1.2 mmol) in THF (30 mL) at -78°C was added a -78°C solution of $[\text{Fe}(\eta^5\text{-C}_5\text{H}_5)(\eta^1\text{-C}_8\text{F}_7)(\text{CO})_2]$ (**17**; 0.28 g, 0.7 mmol)

(35) Plotkin, J. S.; Shore, S. G. *Inorg. Chem.* **1981**, *20*, 284.

(36) Nitay, M.; Rosenblum, M. *J. Organomet. Chem.* **1977**, *136*, C23.

in THF (10 mL) over a 5-min period. After 1 h at -78°C , the solution was warmed to ambient temperature, where it was stirred for an additional 1 h. The anion was then quenched with air and the reaction solvent removed under reduced pressure. The residue was subjected to column chromatography on Florisil. Elution with CH_2Cl_2 (total amount of solvent 100 mL) produced a yellow band. Removal of the solvent under reduced pressure followed by crystallization from CH_2Cl_2 /hexane afforded yellow crystals of **22** (0.09 g, 23%).

Reaction of $\text{K}^+[\text{Fe}(\eta^5\text{-C}_5\text{H}_5)(\text{CO})_2]^-$ with anti-Octa-fluorotricyclo[4.2.0.0^{2,5}]octa-3,7-diene (9). To a stirred solution of **9** (1.01 g, 4.1 mmol) in THF (15 mL) at -78°C was added an orange -78°C solution of $\text{K}^+[\text{Fe}(\eta^5\text{-C}_5\text{H}_5)(\text{CO})_2]^-$ (0.74 g, 3.4 mmol) in THF (15 mL). The reaction mixture was stirred at -78°C for 15 min and warmed to ambient temperature, during which time the solution became red/black. The reaction mixture was then filtered through Celite and the reaction solvent removed under reduced pressure. The residue was subjected to column chromatography on Florisil at 0°C . Elution with CH_2Cl_2 /hexane (20%/80%; total amount of solvent 200 mL) afforded a yellow band. Removal of the solvent under reduced pressure followed by crystallization from CH_2Cl_2 /hexane afforded yellow crystals of **19** (0.28 g, 20%), mp $47\text{--}48^\circ\text{C}$. ^{19}F NMR (CDCl_3): δ 103.6 (m, F_1), 120.5 (m, F_2), 120.8 (m, F_3), 168.8 (m, F_4), 178.6 (m, F_5), 186.0 (m, F_6), 188.1 (m, F_7); $J_{1,4} = 7$, $J_{2,3} = 11$, $J_{2,6} = 11$, $J_{2,7} = 4$, $J_{3,5} = 3$, $J_{3,6} = 4$, $J_{3,7} = 15$, $J_{4,5} = 19$, $J_{4,6} = 7$, $J_{5,7} = 4$, $J_{6,7} = 15$ Hz. ^1H NMR (CDCl_3): δ 5.04 (C_5H_5). IR (Et_2O): $\nu_{\text{CO}} = 2050$, 2002 cm^{-1} ; $\nu_{\text{FC-CF}} = 1757\text{ cm}^{-1}$; $\nu_{\text{FeC-CF}} = 1606\text{ cm}^{-1}$. Anal. Calcd for $\text{C}_{15}\text{H}_5\text{F}_7\text{FeO}_2$: C, 44.37; H, 1.24. Found: C, 44.39; H, 1.37. Elution with CH_2Cl_2 /hexane (45%/55%; total amount of solvent 220 mL) afforded a yellow band containing **20** and **21** (0.72 g, 38%) as a 1:1 mixture of isomers, evidenced by ^{19}F NMR spectroscopy; Mp $181\text{--}183^\circ\text{C}$. IR (Et_2O): $\nu_{\text{CO}} = 2048$, 1995 cm^{-1} . Anal. Calcd for $\text{C}_{22}\text{H}_{10}\text{Fe}_2\text{F}_6\text{O}_4$: C, 46.85; H, 1.79. Found: C, 47.00; H, 1.88. Crystallization at -20°C from CH_2Cl_2 /hexane afforded yellow crystals of one isomer. The assignment of one set of ^1H NMR and ^{19}F NMR resonances to a specific complex was made arbitrarily to facilitate the following discussion. **20**: ^{19}F NMR (CDCl_3): δ 103.0 (m, F_1), 170.5 (m, F_4), 182.1 (m, F_5), 170.5 (m, F_6), 182.1 (m, F_7); ^1H NMR (CDCl_3): δ 5.02 (C_5H_5). Elution with CH_2Cl_2 /hexane (75%/25%; total amount of solvent 100 mL) produced a deep orange band. Removal of the solvent under reduced pressure followed by crystallization from CH_2Cl_2 /hexane afforded yellow crystals of **21**. ^{19}F NMR (CDCl_3): δ 104.7 (m, F_1), 172.8 (m, F_4), 179.7 (m, F_5), 172.8 (m, F_7), 179.7 (m, F_6). ^1H NMR (CDCl_3): δ 5.05 (C_5H_5).

Reaction of $\text{K}^+[\text{Fe}(\eta^5\text{-C}_5\text{Me}_5)(\text{CO})_2]^-$ with OFCOT. The reaction of $\text{K}^+[\text{Fe}(\eta^5\text{-C}_5\text{Me}_5)(\text{CO})_2]^-$ with OFCOT was carried out under conditions similar to those used for the reaction of $\text{K}^+[\text{Fe}(\eta^5\text{-C}_5\text{H}_5)(\text{CO})_2]^-$ with OFCOT described above. Samples of $[\text{Fe}(\eta^5\text{-C}_5\text{Me}_5)(\eta^1\text{-C}_8\text{F}_7)(\text{CO})_2]$ (**24**) (and its bicyclic isomer **25**) and $[\text{Fe}(\eta^5\text{-C}_5\text{Me}_5)(\eta^1\text{-C}_8\text{F}_5\text{O})]$ (**26**) were obtained in an analogous fashion.

Reaction of $\text{Na}^+[\text{Ru}(\eta^5\text{-C}_5\text{H}_5)(\text{CO})_2]^-$ with OFCOT. To a stirred THF (15 mL) solution of OFCOT (0.40 g, 1.6 mmol) at -78°C was added a bright yellow -78°C THF (5 mL) solution of $\text{Na}^+[\text{Ru}(\eta^5\text{-C}_5\text{H}_5)(\text{CO})_2]^-$ (1.5 mmol), prepared in situ from the reaction of $[\text{Ru}(\eta^5\text{-C}_5\text{H}_5)(\text{CO})_2]_2$ (0.33 g, 0.74 mmol) with Na/Hg amalgam, over a 5-min period. The deep black/red solution was stirred at -78°C for 12 h and then warmed to room temperature. The reaction solvent was removed under reduced pressure to afford a red solid. The reaction residue was redissolved in CH_2Cl_2 and filtered through Celite. Crystallization of this solid from CH_2Cl_2 /hexane at -20°C afforded deep yellow crystals of **27** (0.24 g, 36%), mp $92\text{--}94^\circ\text{C}$. ^{19}F NMR (CDCl_3): δ 72.2 (m, F_1), 92.7 (m, F_2), 119.4 (m, F_3), 125.1 (m, F_4), 128.8 (m, F_5), 130.2 (m, F_6), 143.4 (m, F_7); $J_{1,3} = 18$, $J_{3,5} = 25$, $J_{5,6} = 22$, $J_{4,6} = 38$, $J_{4,7} = 23$, $J_{2,7} = 17$, $J_{2,5} = 12$, $J_{3,7} = 11$, $J_{1,4} = 12$, $J_{2,3} = 4$, $J_{5,7} = 3$ Hz. ^1H NMR (CDCl_3): δ 5.36 (C_5H_5). IR (CH_2Cl_2): $\nu_{\text{CO}} = 2049$, 1995 cm^{-1} . MS: m/e 452 (M^+). Anal. Calcd for $\text{C}_{15}\text{H}_5\text{F}_7\text{O}_2\text{Ru}$: C, 39.93; H, 1.12. Found: C, 39.58; H, 1.01. There is an equilibrium in solution between **27** and its bicyclic valence isomer **28** (**28**: ^{19}F NMR (CDCl_3): δ 98.0 (m, F_2), 145.5 (m, F_3), 151.6 (m, F_4), 154.8 (m, F_5), 158.9 (m, F_6), 160.9 (m, F_7); the assignment of the fluorine signals in **28** was made by a comparison with the coupling constants for the isostructural compound **11**.²⁴).

Reactions of $[\text{Fe}(\eta^5\text{-C}_5\text{H}_5)(\eta^1\text{-C}_8\text{F}_7)(\text{CO})_2]$ (17**) with Triphenylphosphine and Triphenylarsine.** To a stirred solution of $[\text{Fe}(\eta^5\text{-C}_5\text{H}_5)(\eta^1\text{-C}_8\text{F}_7)(\text{CO})_2]$ (**17**) in hexane (20 mL) was added triphenylphosphine. The solution was warmed to 40°C to completely dissolve all reactants. The Schlenk flask was then placed 10 cm from the photolysis lamp and irradiated for 2 h. The volume of the reaction solvent was reduced to ~ 10 mL and the solution cooled to 4°C . Filtration of the red solid on a medium-porosity frit followed by a hexane wash (15 mL) produced **29** as a 1:1 mixture of diastereoisomers as indicated by ^{19}F NMR spectroscopy.

A similar reaction of $[\text{Fe}(\eta^5\text{-C}_5\text{H}_5)(\eta^1\text{-C}_8\text{F}_7)(\text{CO})_2]$ (0.75 g, 1.8 mmol) with triphenylarsine (1.41 g, 4.6 mmol) produced **30** (1.0 g, 82%) as a 2:1 mixture of diastereoisomers **a** and **b**. The assignment of one set of fluorine resonances to a specific isomer is arbitrary and was made to facilitate the following discussion. Crystallization of the reaction products twice from CH_2Cl_2 afforded a sample of **30a**: ^{19}F NMR (CDCl_3): δ 71.9 (m, F_1), 87.5 (m, F_2), 117.9 (m, F_3), 121.5 (m, F_4), 128.3 (m, F_5), 130.5 (m, F_6), 145.8 (m, F_7); ^1H NMR (C_7D_8): δ 4.43 (s, C_5H_5); $^{13}\text{C}\{^{19}\text{F}\}$ NMR (C_6D_6): δ 82.2 (d, $J_{\text{CH}} = 180$ Hz, C_5H_5), 220.0 (CO); IR (hexane) $\nu_{\text{CO}} = 1955\text{ cm}^{-1}$. **30b**: ^{19}F NMR (CDCl_3): δ 69.3 (m, F_1), 90.0 (m, F_2), 118.2 (m, F_3), 122.3 (m, F_4), 130.1 (m, F_5), 131.7 (m, F_6), 144.6 (m, F_7); a complete analysis of the coupling constants for an isostructural complex (**27**) appears above, and inspection reveals a similar coupling pattern for **30a** and **30b**.

Crystallographic Analysis. For each experiment a single crystal was affixed to a glass fiber attached to a goniometer head and then transferred to a Syntex P2₁ autodiffractometer, where it was maintained in a cold stream (-110°C) of dry nitrogen gas for the duration of the data collection. Preliminary diffraction studies allowed determination of crystal symmetry and verification of the suitability of the crystals for data collection. A summary of the pertinent crystal data and of details of the X-ray diffraction data collection and processing is presented in Table V. The measured intensities were reduced and assigned standard deviations as described elsewhere,²⁹ including correction for absorption based on crystal shape.

Solution and Refinement of the Structures.³⁷ Each structure was solved by the heavy-atom method, with use of heavy-atom positions determined from a sharpened Patterson map. All structures were refined by full-matrix least-squares methods, with use of the program SHELX76. Neutral-atom scattering factors³⁸ for H, C, O, F, Mn, and Fe were used, including real and imaginary corrections for anomalous dispersion.

In each structure, all non-H atoms were refined anisotropically and any H atoms were individually refined isotropically, except as noted below. Details of the refinements appear in Table V. Each refinement was continued until the shifts in all parameters were less than 1 esd in the respective parameter.

Parallel refinements of **17** with unconstrained isotropic parameters in the two space groups *Cc* and *C2/c* have indicated, by the more unreasonable geometry and more erratic behavior of thermal parameters in all parts of the molecule in *Cc*, that *C2/c* is the correct space group.

In **24**, hydrogen atoms of the methyl groups were constrained to idealized geometry with C-H = 1.00 Å and C-C-C = C-C-H = 109.5° , with individually refined isotropic *U* values.

In the refinement of **22**, the Cp rings were treated as rigid groups with idealized geometry but with U_{iso} for each H fixed at the final isotropic *U* value for the carbon to which it is attached.

The structure of **13** is characterized by disorder within the fluorocarbon fragment. The most satisfactory disorder model is one in which the atoms of the $\text{Mn}(\text{CO})_6$ group, the seven F atoms, and C(1) and C(8) are each at a single site; inside this exterior, the other six ring atoms each occupy a major site (C(2)–C(7) in Figure 3a) and a minor site (C(2B)–C(7B) in Figure 3b). Re-

(37) Riley, P. E.; Davis, R. E. *Acta Crystallogr., Sect. B* 1976, B32, 381. Computer programs used in the data reduction and in the structure refinement and analysis are as detailed in: Gadol, S. M.; Davis, R. E. *Organometallics* 1982, 1, 1607. See the note at the end of the paper regarding the availability of supplementary material.

(38) Scattering factors for H, C, O, and F atoms were used as programmed in SHELX76. Values for Mn and Fe atoms were obtained from: *International Tables for X-ray Crystallography*; Kynoch Press: Birmingham, England, 1974; Vol. IV.

finement of a fully anisotropic model resulted in a site occupancy ratio of 0.631 (5)/0.369 (5). Though the elongated thermal ellipsoids of C(1) and C(8) are suggestive of disorder in these atoms also, no model in which these atoms were treated with partial occupancy was refined successfully.

Acknowledgment. R.P.H. is grateful to the Air Force Office of Scientific Research (Grant AFOSR-86-0075), the National Science Foundation, and the donors of the Petroleum Research Fund, administered by the American Chemical Society, for generous research support. R.E.D.

gratefully acknowledges the support of the Robert A. Welch Foundation (Grant F-233).

Supplementary Material Available: Listings of bond lengths and angles, fractional atomic coordinates and isotropic (or equivalent isotropic) thermal parameters for hydrogen and non-hydrogen atoms, anisotropic thermal parameters for non-hydrogen atoms, and torsion angles for 17, 24, 22, and 13 (37 pages); tables of observed and calculated structure factors (87 pages). Ordering information is given on any current masthead page.

Synthesis, Structures, and Conformational Dynamics of Dicobalt Complexes Containing the Hexafluorodidehydrocyclooctatetraene (Hexafluorocycloocta-3,5,7-trien-1-yne) Ligand. Crystal and Molecular Structures of $[(\text{Co}(\text{L})(\text{CO})_2)_2(\mu_2\text{-}(1\eta,2\eta)\text{-C}_8\text{F}_6)]$ (L = CO, PPh₃, PPhMe₂, PMe₃)

Russell P. Hughes,^{*,1a} Stephen J. Doig,^{1a} Richard C. Hemond,^{1a} Wayne L. Smith,^{1a,2}
Raymond E. Davis,^{*,1b} Steven M. Gadol,^{1b} and Katherine D. Holland^{1b}

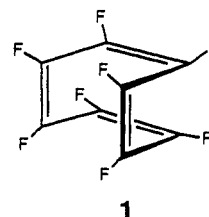
*Chemistry Departments, Dartmouth College, Hanover, New Hampshire 03755,
and University of Texas at Austin, Austin, Texas 78712*

Received March 8, 1990

The reactions of the cobalt anions $[\text{Co}(\text{CO})_3\text{L}]^-$ or the neutral dimers $[\text{Co}_2(\text{CO})_6\text{L}_2]$ (L = CO, PPh₃, PPhMe₂, PPh₂Me, PMe₃, P(*p*-tolyl)₃) with octafluorocyclooctatetraene (OFCOT; 1) afford the dinuclear μ -hexafluorocyclooctatrienyl complexes 4, together with mononuclear η^1 -heptafluorocyclooctatetraenyl complexes 7, which are in equilibrium with their heptafluorobicyclo[4.2.0]octatrienyl valence isomers 8. The conformation of the μ -hexafluorocyclooctatrienyl rings in the four complexes 4 (a, L = CO; b, L = PPh₃; c, L = PPhMe₂; d, L = PMe₃) has been shown by X-ray crystallographic studies to vary from puckered to planar as the steric bulk of the ligands on the adjacent cobalt atoms increases. Evidence of a weak attractive interaction between the bridging fluorinated ligand and phenyl rings of PPh₃ and PPhMe₂ is also presented. Solution NMR studies show that both the steric and electronic interactions are weak. A discussion of the relative barriers to ring inversion in μ -hexafluorocyclooctatrienyl and η^1 -heptafluorocyclooctatetraenyl ligands is presented. X-ray data were collected on a Syntex P2₁ autodiffractometer at -110 °C, and structures were refined by the full-matrix least-squares method. Crystal data for 4a: $a = 26.808$ (6) Å, $b = 6.953$ (1) Å, $c = 17.081$ (3) Å, $\beta = 98.10$ (1)°, monoclinic $C2/c$, $Z = 8$, $R = 0.026$, $R_w = 0.030$ for 3145 reflections with $F_o \geq 4\sigma(F_o)$. Crystal data for 4b: $a = 20.670$ (4) Å, $b = 10.038$ (2) Å, $c = 21.556$ (4) Å, $\beta = 108.14$ (2)°, monoclinic, $C2/c$, $Z = 4$, $R = 0.055$, $R_w = 0.053$ for 3270 reflections with $F_o \geq 4\sigma(F_o)$. Crystal data for 4c: $a = 10.475$ (4) Å, $b = 16.604$ (5) Å, $c = 8.637$ (2) Å, $\alpha = 99.16$ (3)°, $\beta = 91.16$ (2)°, $\gamma = 85.74$ (2)°, triclinic, $P\bar{1}$, $Z = 2$, $R = 0.034$, $R_w = 0.036$ for 6053 reflections with $F_o \geq 4\sigma(F_o)$. Crystal data for 4d: $a = 7.799$ (2) Å, $b = 28.071$ (7) Å, $c = 10.856$ (2) Å, $\beta = 98.40$ (2)°, monoclinic, $P2_1/c$, $Z = 4$, $R = 0.048$, $R_w = 0.038$ for 4482 reflections with $F_o \geq 4\sigma(F_o)$.

Introduction

Nonplanar ground-state structures for cyclooctatetraene and most of its derivatives are well established.³ Crystallographic studies of the perfluorinated analogue octafluorocyclooctatetraene (OFCOT; 1) have shown that fluorination does not result in significant alteration of the skeletal structure.⁴ The question of whether the corre-



(1) (a) Dartmouth College. (b) University of Texas at Austin.
(2) ACS-PRF Summer Faculty Fellow on Sabbatical leave from the Chemistry Department, Colby College, Waterville, ME 04901.
(3) For reviews of the organic and organometallic chemistry of cyclooctatetraene see: (a) Fray, G. I.; Saxton, R. G. *The Chemistry of Cyclooctatetraene and Its Derivatives*; Cambridge University Press: Cambridge, England, 1978. (b) Deganello, G. *Transition Metal Complexes of Cyclic Polyolefins*; Academic Press: New York, 1979.

sponding dehydro[8]annulenes (cycloocta-3,5,7-trien-1-yne) should be planar or puckered has aroused considerable experimental and theoretical interest. Experimental evidence has been presented for the existence of di-

(4) Laird, B. B.; Davis, R. E. *Acta Crystallogr., Sect. B* 1982, B38, 678.